PILLARED CLAYS AS SUPERIOR CATALYSTS FOR SELECTIVE CATALYTIC REDUCTION OF NITRIC OXIDE

DE-FG22-96PC96206

Semi-Annual Technical Progress Report
September 1, 1996 - February 28, 1997

submitted to

Dr. William P.Barnett
U.S. Department of Energy
Pittsburgh Energy Technology Center
P.O. Box 10940 MS 922-273C
Pittsburgy, PA 15236-0940

by

Ralph T. Yang

Authors: W. B. Li, M. Sirilumpen, N. Tharapiwattananon and R. T. Yang
Deaprtment of Chemical Engineering
University of Michigan
Ann Arbor, MI 48109-2136

DISCLAIMER

SUMMARY

During the first six months of the program, the work has progressed as planned. We have constructed a reactor system and assembled all laboratory essentials for conducting the three-year project.

First, the catalytic activities of the Cu^{2+} ion-exchanged alumina-pillared clay for the selective catalytic reduction of NO by ethylene were measured. The temperature range was 250 - 500°C. The activities of this catalyst were substantially higher than the catalyst that has been extensively studied in the literature, Cu-ZSM-5. Fourier-Transform Infrared Spectroscopy (FTIR) was used to study the acidity of the catalyst. The second part of the work was an in-depth FTIR study of the NO decomposition mechanism on the catalyst. This was planned as the first and the key step to obtain an understanding of the reaction mechanism. Key surface intermediates were identified from the FTIR spectra, and a redox type Eley-Rideal mechanism was proposed for the NO decomposition on this catalyst.

This report will be divided into two parts. In Part One, we report results on the catalytic acitvities of the Cu-alumina-pillared clay and a direct comparison with other known catalysts. In Part Two, we focuse on the FTIR study and from the results, we propose a NO decomposition mechanism on this new catalyst.

Plans for the next six months include tests of different pillared clays as well as the catalytic mechanism. The micro reactor will continue to be the key equipment for measuring the catalytic activities. FTIR will continue to be the major technique for identifying surface species and hence understanding the reaction mechanism.

Part One Selective Catalytic Reduction of NO by Ethylene on Cu^{2+} Ion-Exchanged Alumina-Pillared Clay

ABSTRACT

Cu^{2+} ion-exchanged pillared clays are substantially more active than Cu^{2+}-ZSM-5 for selective catalytic reduction (SCR) of NO by hydrocarbons. More importantly, H_2O (or SO_2) has only mild effects on their activities. First results on Cu^{2+} exchanged TiO_2-pillared montmorillonite were reported in our earlier work (Yang and Li, J. Catal., **154 (1995)** 414), that showed overall activities two to four times higher than Cu^{2+} -ZSM-5.

A delaminated pillared clay was subjected to Cu^{2+} ion-exchange and studied for SCR by C_2H_4 in this work. The Cu^{2+} ion-exchanged delaminated Al_2O_3-pillared clay yielded substantially higher SCR rates than both Cu^{2+} exchanged TiO_2-pillared clay and Cu^{2+}-ZSM-5 at temperatures above 400 °C. The peak NO conversion was 90% at 550 °C and at a space velocity of 15,000 h^{-1} (with O_2=2%). The peak temperature decreased as the concentration of O_2 was increased. The macroporosity in the delaminated pillared clay was partially responsible for its higher peak temperatures (than that for laminated pillared clays). At 1000 ppm each for NO and C_2H_4, the NO conversion peaked at 2% O_2 for all temperatures. H_2O and SO_2 caused only mild deactivation, likely due to competitive adsorption (of SO_2 on Cu^{2+} sites and H_2O on acid sites). The high activity of Cu^{2+} exchanged Al_2O_3-pillared clay was due to a unique combination of the redox property of the Cu^{2+} sites and the strong Lewis acidity of the pillared clay. The suggested mechanism involved NO chemisorption (in the presence of O_2) on Cu^{2+}-O-Al^{3+}- on the pillars, and C_2H_4 activation on the Lewis acid sites to form an oxygenated species.

INTRODUCTION

Selective catalytic reduction (SCR) of NO by NH_3 is presently performed with vanadia-based catalysts for flue gas applications[1]. Hydrocarbons would be the preferred reducing agents over NH_3 because of the practical problems associated with the use of NH_3 (i.e., handling and slippage through the reactor). SCR of NO by hydrocarbon can also find important applications for lean-burn (i.e., O_2-rich) gasoline and diesel engines where the noble-metal three-way catalysts are not effective in the presence of excess oxygen [2,3].

The first catalysts found to be active for SCR of NO by hydrocarbons in the presence of oxygen were Cu^{2+} ion-exchanged ZSM-5 and other zeolites, reported in 1990 by Iwamoto[4] and Held et al. [5] and in early patents cited in [6]. Reports on a large number of catalysts for this reaction have appeared since 1990. The majority of these catalysts are ion-exchanged zeolites, including H^+ forms. Alumina and metal oxides supported on alumina have also been studied, but are less active. The early (1990-1992) literature on the subject, primarily by Japanese researchers, has been reviewed by Iwamoto and Mizuno [7] and will not be repeated here. The most active catalysts include: Cu-ZSM-5[2,4,5,8-14], Co-ZSM-5 and Co-Ferrierite [15-18], Ce-ZSM-5 [6,19], Pt/X zeolite [20], Cu-Zr-O and Cu-Ga-O [21,22]. Although Cu-ZSM-5 is the most active catlayst, it suffers from severe deactivation in engine tests, presumably due to H_2O and SO_2 [23-25]. A comprehensive review and discussion on the reaction was made recently by Shelef [26].

Pillared clays are two-dimensional zeolite-like materials prepared by exchanging charge-compensating cations between the clay layers with large inorganic metal hydroxycations, which are oligomeric and are formed by hydrolysis of metal oxides or salts [27]. Upon heating, the metal hydroxycations are decomposed into oxide pillars which keep the clay layers apart and create zeolite-like interlayer and interpillar spaces. Since pillared clays have a number of attractive features such as porosity, high thermal stability and exchangeable acidity, they have been widely studied as catalysts [28-30] and as adsorbents[31,32].

Delaminated pillared clay is one class of pillared clay, which was first synthesized by Pinnavaia et al. [33]. Delaminated pillared clays do not exhibit long-range layer stacking, as shown by the absence of the (001) X-ray reflections. However, the short-range stacking with a pillared structure still exists, and the overall structure is best described as "house-of-cards"[33,34]. These clays contain both micropores and macropores; the latter do not exist in the laminated pillared clays. The introduction of macropores can significantly increase the diffusion rates, hence the overall activities as well as the kinetic behavior are affected (as will be shown in this work). As with zeolites, catalysis by modification of pillared clays with transition metal ions is a field rich for exploitation. When pillared clays are modified (by ion-exchange or doping) by transition metal ions, some unique catalytic properties for certain reactions were observed. For example, metal ion exchanged alumina pillared clays have high activities for glycol ether production from epoxide and ethanol [35].

We have recently reported first results on the high activities of Cu^{2+} ion-exchanged TiO_2-pillared clay for SCR of NO by ethylene [36]. We have also reported high SCR

activities by pillared clays ion-exchanged with Fe^{3+} or other transition metal ions and Fe_2O_3-pillared clays [37, 38] for SCR with NH_3.

In this work, Cu^{2+} ion-exchanged delaminated pillared clays were studied for SCR of NO with ethylene. The higher SCR activities (as compared with Cu^{2+} exchanged pillared clays) are clearly shown, particularly in the high temperature range, i.e., above 400 °C. We first investigated the SCR activity over Cu^{2+} -exchanged delaminated laponite. The effect of O_2 on the SCR activity was then investigated, since oxygen is an important factor for NO reduction by NH_3 [1] and by hydrocarbon [7]. In addition, effects of water vapor and sulfur dioxide were also studied. Finally, a mechnism was described for NO reduction by ethylene in the presence of oxygen on Cu^{2+} ion-exchanged pillared clays.

EXPERIMENTAL

The syntheses of the three catalysts are first described.

Synthesis of Cu^{2+}-Exchanged Al_2O_3-Pillared Laponite

Delaminated Al_2O_3-pillared laponite used in the synthesis was obtained from Laporte Industries, Ltd. Prior to use, it was suspended as 1% (by weight) slurry and washed with dilute NH_4NO_3 solution to remove impurities and existing metal ions. After filtration, the residue was dried at 110°C in air. Then it was again suspended as 1% (by weight) slurry. 10 ml of 0.1M $Cu(NO_3)_2$ solution was added to 100 ml of the above slurry, with constant stirring. The acidity of the mixture was adjusted to pH = 5.5 by using ammonium hydroxide and nitric acid solutions. The mixture was then kept at 50°C for 6 h. Subsequently, the residue was thoroughly washed with distilled water 5 times. The obtained solid sample was first dried at 110°C in air for 24 h, then crushed and sieved to collect the desired size fractions. The samples were further heated to 400 °C in air, and were kept at this temperature for 12 h. After these pretreatments, the samples were ready for further experiments. The BET N_2 surface area for the delaminated Al_2O_3 pillared laponite was 384 m^2/g, and that of the Cu^{2+} ion-exchanged form was 360 m^2/g.

Cu^{2+} Exchanged TiO_2-Pillared Bentonite Clay

Cu^{2+} exchanged TiO_2 pillared bentonite clays were prepared by ion exchange of TiO_2-pillared clays with copper nitrate solution following the conventional ion exchange procedure. TiO_2-pillared clay was prepared from a purified montmorillonite (bentonite) powder (from Fisher, with crystal sizes less than or equal to 2 mm) and titanium chloride

($TiCl_4$, also from Fisher) following the procedure of Sterte [39]. One gram of the obtained TiO_2-pillared clay was added to 100 ml of 0.02 M copper nitrate solution. The mixture was stirred for 24 h at 70°C. The pH of the starting solution was adjusted to pH = 6.0 by adding proper amounts of ammonia solution. The ion-exchanged product was collected by filtration followed by washing with distilled water five times. The detailed procedure has been described in our previous paper [36]. The same pretreatment as that for the Cu^{2+}-exchanged Al_2O_3-pillared laponite was made before the samples were ready for catalytic activity experiments.

Cu^{2+}-Exchanged ZSM-5

The Cu^{2+}-exchanged ZSM-5 was prepared by mixing the ZSM-5 sample (kindly supplied by Exxon Company) with an aqueous solution of cupric nitrate. The silica/alumina ratio in the ZSM-5 was 30. Before ion exchange, the ZSM-5 was washed in 0.01 M $NaNO_3$ solution. After washing, 2 g of ZSM-5 was added to 100 ml of 0.01 M cupric nitrate aqueous solution, with constant stirring for 12 h. The sample was collected after the resulting suspension was filtered, washed, and dried at 110°C. The detailed procedure was described by Sato et al. [40]. The same pretreatment was also made before the samples were ready for catalytic experiments.

Apparatus and Gases Used

The SCR activity measurements were carried out in a fixed-bed quartz reactor. The reaction temperature was controlled by an Omega (CN-2010) programmable temperature controller. The catalyst was supported on a fritted support. The typical reactant gas composition was as follows: NO = 1,000 ppm; 1,000 ppm of ethylene; 0% - 4% of oxygen; 500 ppm of SO_2 (when used); 5% of water vapor (when used), and balance of N_2. The total flowrate was 250 cm^3/min (ambient conditions). The catalyst size fraction was 80 - 100 US mesh, and 0.5 g was used in a typical experiment. The premixed gases (0.7% NO in N_2, 1.04% ethylene in N_2 and 1.0% SO_2 in N_2) were supplied by Matheson Company. The NO concentration was continuously monitored by a chemiluminescent NO/NO_x analyzer (Thermo Electron Corporation, Model 10). Details of the apparatus system for the SCR reaction have been described elsewhere [41]. Product analysis for N_2 and N_2O for the Cu^{2+}exchanged pillared clay showed no N_2O in our earlier study [36]. No product analysis was performed in this work.

RESULTS AND DISCUSSION

Comparison of Activities of Cu^{2+}-Exchanged Delaminated Al_2O_3-Pillared Clays, Cu^{2+}-Exchanged TiO_2-Pillared Clays and Cu^{2+} -Exchanged ZSM-5

Cu^{2+}-exchanged ZSM-5 is a most active and most extensively studied catalyst for hydrocarbon SCR. We have recently reported first results on Cu^{2+}-exchanged TiO_2-pillared clays and showed that they are more active (by two to four times) than Cu^{2+}-exchanged ZSM-5 [36]. Figure 1 compares the results of three catalysts for SCR with C_2H_4 in O_2 - the two mentioned above and Cu^{2+}-exchanged Al_2O_3 delaminated pillared laponite clay. These three catalysts were compared under identical reaction conditions. The results showed that at temperatures higher than 350°C, Cu^{2+}-exchanged delaminated Al_2O_3-pillared laponite clay was much more active than the two other catalysts. The catalytic behavior for the SCR reaction of Cu^{2+}-exchanged delaminated Al_2O_3-pillared laponite is unique in two ways; the peak temperature is higher (at 550°C) and the activities are higher at temperatures above 350°C. This unique behavior is related to its pore structure and its surface acidity. These two aspects (pore structure and surface acidity) are discussed separately below.

Pore Structure of Delaminated Pillared Clay

Laponite is a synthetic hectorite with relatively small particle size (0.05 mm dimension), as compared with the size of natural hectorite or montmorillonite (2.0 mm dimension) [42]. The small crystal size of laponite results in relatively more edge area than face area as compared to clays with larger sizes. Clays are known to flocculate in aqueous suspension by three different modes of association, i.e. edge-to-edge, edge-to-face, and face-to-face [43]. Clays exchanged with polyhydroxy metal cations also undergo association via these three modes.

The Al_2O_3 delaminated laponite was composed of micropores as well as a considerable amount of macropores, as shown by Pinnavaia et al. [33]. The edge-to-edge interactions of layers lead to the formation of macropores with dimensions larger than 3 nm. Some face-to-face aggregation also occurs that involves only 2-4 layers, which leads to the formation of micropores of dimensions 0.5-15 nm, as in laminated pillared clays. This short range stacking is not detected by x-ray diffraction, and thus a mixed laminated/delaminated structure is x-ray amorphous. The absence of distinct x-ray

reflections in the XRD pattern of Cu^{2+}-exchanged Al_2O_3-laponite (Figure 2A) indicated delamination of the sample.

In contrast, XRD of Cu^{2+}-exchanged TiO_2-pillared clay (shown in Figure 2B) and Cu^{2+}-exchanged ZSM-5 (shown in Figure 2C) exhibit crystalline x-ray diffraction patterns. Both of these have only micropore structures [36]. Therefore, both macropores and micropores in Cu^{2+}-exchanged Al_2O_3-delaminated laponite can readily allow hydrocarbon and nitric oxide molecules to reach the interior active sites. In addition, they have higher surface areas, that is, 384 m^2/g and 360 m^2/g for delaminated alumina-pillared laponite and its Cu^{2+}-exchanged form, respectively.

The peaking of NO conversion at a certain temperature for SCR is the result of two competing reactions: NO reduction by hydrocarbon, and oxidation of hydrocarbon that depletes the reductant. In addition, it is known that SCR reaction in molecular sieving catalysts is significantly limited by pore diffusion resistance [2, 12, 36]. The diffusion rates of both reactant and product molecules may play a role in the overall rate. The temperature dependence is different for pore diffusion in macropores and in micropores. Diffusion in ZSM-5 (with channel dimensions of the order of 5 Å) is an activated process, thus its temperature dependence is weaker than being proportional to $T^{0.5}$ (proportional to $T^{0.5}$ being for Knudsen diffusion). Diffusion in macropores, as in the delaminated pillared clay, has a temperature dependence in the range of being proportional to T to $T^{1.5}$. The stronger (or sharper) temperature dependence for diffusion in the delaminated clay will give rise to a higher peak temperature for the overall rate. The relationship is illustrated qualitatively in Figure 3. This is only a partial reason for the higher temperature peak for SCR in delaminated clay. Another possible reason, a chemical reason, is given in the discussion to follow.

Reaction Mechanism

Our data showed that Cu^{2+}-exchanged delaminated Al_2O_3-pillared laponite is highly active. SCR activity was also measured for the Al_2O_3-pillared laponite clay without Cu^{2+} exchange, and the sample without Cu^{2+} showed no activity. Cu^{2+} ions clearly play an important role in this reaction. Therefore, it is helpful to understand the location of the Cu^{2+} ions in the Cu^{2+}-exchanged Al_2O_3-pillared clay in order to gain insight into the

reaction mechanism. The literature information on the actual location of metal ions in ion-exchanged pillared clays is scarce. It is generally thought that mobile metal ion species exist between the clay layers to compensate the charges of the clay layers [30], and that the locations are different for different cations.

For cupric ion sites in the Cu^{2+}-exchanged alumina pillared clay, Kukkadapu and Kevan [44], used ESR (Electron Spin Resonance) and ESEM (Electron Spin Echo Modulation) techniques to study the Cu^{2+} species and assigned the Cu^{2+} as a distorted octahedral species attached to the Al_{13} oligomeric pillar by displacement of water ligands. The basis of their assignment was that the observed ESR parameters were similar to that of $Cu(H_2O)_6^{2+}$ chemisorbed on -Al-OH groups of aluminum hydroxide, and was most characteristic of distorted octahedral symmetry. Consequently, they indicated that the Cu^{2+} ion was linked directly with four water molecules, two of which coordinated axially at a greater distance and the other two bonded equatorially at a shorter distance. The remaining two equatorial coordination positions were occupied by alumina pillar species.

A similar conclusion was reported recently by Bergaoui et al. [45] by using adsorption isotherm and EPR techniques to study Cu^{2+} ion sites on both wet and dry Cu^{2+} alumina pillared saponite. They confirmed that Cu^{2+} was directly bonded to surface (Al-O) groups on alumina pillars similar to Cu^{2+} chemisorbed on bulk alumina phases, and that there was no mobile ion-exchanged $Cu(H_2O)_6^{2+}$ present in the interlayer region.

Note that all these studies were performed at temperatures below 200°C. The Cu^{2+}-exchanged pillared laponite clays in our SCR reaction system were subjected to higher temperatures. The Cu^{2+}-exchanged alumina pillared laponite will undergo further dehydration and dehydroxylation at higher temperatures (than 200°C) and change its coordination state (Kukkadapu and Kevan, 46). However, based on their results [46], it is likely that the Cu^{2+} species in our SCR reaction system was directly bonded to alumina pillars as Cu^{2+}-O-Al^{3+} on the catalyst rather than existing as a mobile species. We use the term "ion exchanged" to describe the catalyst due to the procedure by which the sample was prepared. Such a structure is favorable for dispersion of Cu^{2+} ions in Cu^{2+}-exchanged alumina pillared laponite. Furthermore, the high SCR activity was likely the result of such Cu^{2+} species that combined with the acidity of the pillared clay, as discussed below.

It is known that pillared clays have both Lewis and Brönsted acidities [47]. The acidity of Cu^{2+}-exchanged alumina pillared laponite is shown by IR spectra of chemisorbed NH_3, Figure 4. The IR spectra were measured with a self-supporting pellet of the sample after ammonia adsorption at 25°C, followed by helium purge at increasing temperatures. The strong absorption bands at 1640 cm^{-1} can be assigned to the bending mode of ammonia molecules coordinated on Lewis acid sites, whereas the band at 1455 cm^{-1} is the characteristic absorption due to ammonium ions on Bronsted acid sites [48]. The intensities of both 1640 cm^{-1} and 1455 cm^{-1} bands decreased as temperature was increased. When the temperature was increased to 410°C, the intensity of the 1455 cm^{-1} band nearly vanished and that of 1640 cm^{-1} band remained strong. This result indicates that Lewis acid sites were dominant in the Cu^{2+}-exchanged alumina pillared laponite at high temperatures. The result is in line with that of Yamanaka et al. [49] and He et al. [47].

Based on the understanding of the structure and the acidity of the Cu^{2+}-exchanged delaminated Al_2O_3-pillared laponite, it is clear that the support acidity and the metal ion (Cu^{2+}) redox property both play a significant role in the SCR reaction mechanism. It is proposed that ethylene chemisorbs on the Lewis acid sites on the Cu^{2+}-exchanged alumina pillared laponite. The ethylene molecule is activated and forms oxygenated species in the presence of oxygen, since it is known that alkenes complex with alumina by Al^{3+}-O^{2-} ionic pairs as identified by IR specroscopy (Gordymova and Davydov, cited in 50). At the same time, NO adsorbs on the Cu^{2+} ion sites which are bonded to the alumina pillars. The obtained oxygenated hydrocarbon intermediates and the adjacent chemisorbed NO further react to form nitrogen-containing hydrocarbon-oxygenated intermediates on the conjugated Al-O-Cu sites. These intermediates further decompose into nitrogen and carbon dioxide. The activity of the oxygenated hydrocarbon intermediate is related to the acidity, and the Cu^{2+} ion redox property is responsible for the activity of the adsorbed NO. Both the acidity and the Cu^{2+} ion redox property are important for the overall activity. Since Cu^{2+} ions are anchored on the alumina pillars in the Cu^{2+}-exchanged alumina pillared laponite, these two factors combine well to yield the high SCR activity. The alumina pillars bonded to the silica-clay layer surfaces provide the Lewis acid sites that are needed for the reaction [26]. The importance of the support in the SCR reaction has been noted by Cho [51] and

Shelef [26]. For the CH_4+NO+O_2 reaction on Co-ZSM-5, an isocyanate (NCO) intermediate has been identified [52].

Now we return to the experimental data. Increasing the reaction temperature resulted in a mild decrease in Lewis acidity. The Lewis acidity still remained high enough at the SCR reaction temperatures as shown in Figure 4. Meanwhile, increasing temperature also increased the activity of the oxygenated hydrocarbon intermediates on the Lewis sites. Thus, at high temperatures the oxygenated hydrocarbon intermediates readily reacted with the chemisorbed NO species on adjacent Cu^{2+} ion sites. Oxygen was necessary (as will be discussed shortly) in the reaction. However, significant ethylene oxidation occurred on the surface at still higher temperatures that decreased the SCR rates, as already discussed.

Effect of O_2 on SCR Activity Over Cu^{2+} Ion Exchanged Al_2O_3-Pillared Laponite.

It is known that oxygen is important in SCR reactions both by hydrocarbon (e.g., over Cu^{2+}-ZSM-5, 4) and by NH_3 (i.e., over V_2O_5/TiO_2, 1). The effect of O_2 on SCR by C_2H_4 over Cu^{2+}-exchanged Al_2O_3-pillared laponite was studied, and the results are shown in Figure 5. Figure 5 shows NO conversion as a function of oxygen concentration over Cu^{2+}-exchanged Al_2O_3-pillared laponite at various temperatures. In the absence of oxygen, no or little activity was seen, as shown in Figure 5. At all reaction temperatures studied, NO conversion increased significantly with oxygen concentration, up to 2% O_2, followed by a slight decrease at 4% O_2.

Figure 5 also shows the shifting peak temperature for the reaction with O_2 concentration. For example, the temperature for the peak activity at 2% O_2 was 550°C, whereas it shifted to 450 °C at 4% O_2. This was the direct result of C_2H_4 oxidation that was more severe at 4% O_2. Similar O_2 effects were reported recently by Cho [51] using transient techniques for SCR of NO by ethylene over Cu-ZSM-5. The O_2 effect is clearly important in applications for design for optimal operation.

Effects of H_2O and SO_2 on NO SCR by C_2H_4 on Cu^{2+} Exchanged Pillared Laponite.

Although Cu^{2+}-ZSM-5 has been the most extensively studied catalyst for SCR of NO by hydrocarbons, it suffers from severe and rapid deactivation by exposure to low concentrations of H_2O [25]. Our preliminary results [36] showed that Cu^{2+} exchanged pillared clay was stable over a testing period of 48 hrs. and that , more importantly, H_2O and SO_2 decreased its SCR activity only slightly. The effects of H_2O and SO_2 were studied separately on the Cu^{2+} exchanged delaminated Al_2O_3-pillared clay.

Effects of H_2O and SO_2 on the SCR activity are shown in Figure 6. The activity was decreased only mildly at 500 °C. The deactivation became stronger toward lower temperatures , and were quite severe at 350 °C.

The reason for deactivation was possibly due to competitive adsorption for the active sites, as discussed for SCR by NH_3 on V_2O_5/TiO_2 [54, 55] and for SCR by CH_4 on Co-ferrierite[53]. Support for this mechanism was obtained from the following experiments. The catalyst was first saturated by NO (1000 ppm) at both room temperature and at 300 °C. The sample was then purged with N_2. The sample was subsequently exposed to SO_2 (500 ppm) in N_2, and considerable amounts of NO were desorbed at both temperatures as detected by the chemiluminescent NO anlyzer. This result indicated that SO_2 adsorbed on the same sites as that by NO. On the other hand, no NO was detected when H_2O (5%) was introduced. This result indicated that the sites for H_2O adsorption were different from that for NO, i.e. ,deactivations by H_2O and SO_2 were different. It is possible that H_2O changed the acidity and hence the SCR activity.

REFERENCES to PART ONE

1. H. Bosch and F. Janssen, *Catal. Today* **4** (1989) 369.
2. B. K. Cho, *J. Catal.* **142** (1993) 418.
3. K. C. Taylor, in "Catalysis: Science and Technology" (J. R. Anderson and M. Boudart, Eds.), Vol. 5, Springer-Verlag, Berlin, 1984.
4. M. Iwamoto, "Symposium on Catalytic Technology for Removal of Nitrogen Oxides," pp. 17-22, Catal. Soc. Japan (1990).
5. W. Held, A. König, T. Richter and L. Puppe, SAE Paper 900,469 (1990).
6. C. Yokoyama and M. Misono, *J. Catal.* **150** (1994) 9.
7. M. Iwamoto and N. Mizuno, *Proc. Inst. Mech. Eng. Part D, J. Auto. Eng.*, **207** (1993) 23.
8. J. Valyon and W. K. Hall, *J. Catal.* **143** (1993) 520.
9. J. Petunchi, G. A. Sill and W. K. Hall, *Appl. Catal.* **B 2** (1993) 303.

10. A. P. Ansell, A. F. Diwell, S.E. Colunski, J. W. Hayes, R. R. Rajaran, T. J. Truex and A. P. Walker, *Appl. Catal.* **B 2** (1993) 101.
11. C. H. Bartholomew, R. Gopalakrishnan, P. R. Stafford, J. E. Davison and W. C. Hecker. *App. Catal.* **B 2** (1993) 183.
12. Y. Li and J. N. Armor, *Appl. Catal.* **B 3** (1994) L1.
13. D. J. Liu and H. J. Robota, *Appl. Catal.* **B 4** (1994) 155.
14. Z. Chajar, M. Primet, H. Praliaud, M. Chevrier, C. Gauthier and F. Mathis, *Appl. Catal.* **B 4** (1994) 199.
15. Y. Li and J. N. Armor, *Appl. Catal.* **B 1** (1992) L 31.
16. F. Witzel, G. A. Sill and W. K. Hall, *J. Catal.* **149** (1994) 229.
17. a. Y. Li and J. N. Armor, *J. Catal.* **150** (1994) 376.
b. Y. Li, T. L. Slager and J. N. Armor, *J. Catal.* **150**(1994) 388.
18. Y. Zhang, A. Patwardhan, Z. Li, A. Sarofim and M. Flytzani-Stephanopoulos, paper presented at AIChE Annual Meeting, Paper 82f, Miami, FL, Nov. 15 (1995).
19. M. Misono and K. Konodo, *Chem. Lett.* **1001**(1991).
20. Amiridis, M., and Pereira, C., paper presented at AIChE Annual Meeting, Paper 61h, Miami, FL, Nov. 14(1995).
21. K. A. Bethke, D. Alt, and M. C. Kung, *Catal. Lett.* **25** (1994) 37.
22. M. Kung, K. Bethke, D. Alt, B. Yang and H. Kung, in "NOx Reduction," (U. S. Ozkan, S. Agarwal and C. Marcelin, Eds.), Chap. XX, ACS Symp. Ser., ACS. Washington, DC, 1995.
23. M. J. Heimrich and M. L. Deviney, SAE Paper 930, 736 (1994).
24. D. R. Monroe, C. L. DiMaggio, D. D. Beck, and F. A. Matekunas, SAE Paper SP-930 (1994) 737.
25. J. N. Armor, *Appl. Catal.* **B 4** (1994) N18.
26. M. Shelef, *Chem.Rev.* **95** (1995) 209.
27. C. F. Baes and R. E. Mesmer, The Hydrolysis of Cations, Wiley, New York (1976).
28. T. J. Pinnavaia, *Science*, **220** (1983) 365.
29. F. Figueras, *Catal. Rev. Sci. Eng.*, **30** (1988) 457.
30. R. Burch Ed., *Catalysis Today*, **2** (1988) 185, Elsevier, New Yok.
31. R. T. Yang and M. S. A. Baksh, *AIChE J.*, **37** (1991) 679.
32. L. S. Cheng and R. T. Yang, *Ind. Eng. Chem. Res.*, **34**, 2021 (1995).
33. T. J. Pinnavaia, M-S. Tzou, S. D. Landau, and R. Raythatha, *J. Mol. Catal.*, **27** (1984) 195.
34. M. L. Occelli, S. D. Landau, and T. J. Pinnavaia, *J. catal.* **104** (1987) 331.

35. M. P. Atkins, in "Pillared Layered Structures. Current Trends and Applications" , I. V. Mitchell Ed., Elsevier, New York (1990), p.159.
36. R. T. Yang and W. B. Li, *J. catal.* **155** (1995) 414.
37. R. T. Yang, and J. E. Cichanowicz, Pillared Interlayered Caly Catalysts for the Selective Catalytic Reduction of Nitric Oxide with Ammonia, U.S. Patent 5,415,850 (1995).
38. J. P. Chen, M.C. Hausladen and R. T. Yang, *J. Catal.* **151** (1995) 135.
39. J. Sterte, *Clays and Clay Minerals*, **34(6)** (1986) 658.
40. S. Sato, Y. Yu-u, H. Yahiro, N. Mizuno and M. Iwamoto, *Appl. Catal.*, **70** (1991) L1.
41. R. T. Yang, J. P. Chen, E. S. Kikkinides, L. S. Cheng, and J. E. Cichanowicz, *Ind. Eng. Chem. Res.*, **31** (1992) 144.
42. H. Van. Olphen, J. J. Fripiat Eds., Data Handbook for Clay Minerals and Other Non-Metallic Minerals, Pergamon, Oxford (1979), p.41.
43. H. Van. Olphen, An Introduction to Clay Colloid Chemistry, Wiley, New York (1977), p.95.
44. R. K. Kukkadapu and L. Kevan, J. Phys. Chem., 93 (1989) 1654.
45. L. Bergaoui, J-F. Lamber, H. Suquet and M. Che, *J. Phys. Chem.*, **99** (1995) 2155.
46. R. K. Kukkadapu and L. Kevan, *J. Phys. Chem.*, **92** (1988) 6073.
47. M.Y. He, Z. Liu and E. Min, *Catal. Today*, **2** (1988) 321.
48. M. C. Kung and H. H. Kung, *Catal. Rev. - Sci. Eng.*, **27** (1985) 425.
49. S. Yamanaka, T. Nishihara, M. Hattori, in " Microstructure and Properties of Catalysts," M. M. J. Treacy, J. M. Thomas, J. M. White Eds., Materials Research Society, Pittsburgh, PA (1988), p.283.
50. A. A. Davydov, Infrared Spectroscopy of Adsorbed Species on the Surface of Transition Metal Oxides, Wiley, New York (1990), P. 151.
51. B.K. Cho, *J. Catal.*, **155** (1995) 184.
52. A. W. Aylor, L. J. Lobree, J. A. Reimer and A. T. Bell, paper presented at AIChE Annual Meeting, Miami, FL., Nov. 15, 1995, paper 82e.
53. Y. Li, J. N. Armor, *Appl. Catal.* **B 5** (1995) L257.
54. J. P. Chen, and R. T. Yang, *J. Catal.*, **125** (1990) 411.
55. N. Y. Tøpsoe, T. Slabiak, B. S. Clausen, T. Z. Srnak and J. A. Dumesic, *J. Catal.*, **134** (1992) 742.

Figure Captions:

Figure 1. SCR activity over (A) Cu^{2+}-exchanged delaminated Al_2O_3-pillared laponite, (B) Cu^{2+}-exchanged TiO_2-pillared bentonite, and (C) Cu^{2+}-exchanged ZSM-5. NO = 1,000 ppm, C_2H_4 = 1,000 ppm, O_2 = 2%, catalyst = 0.5 g, N_2 = balance, total flowrate = 250 cc/min, space velocity=15,000 h^{-1}. Note for catalyst A, the NO conversion peaks at 90% at 550 °C and drops to 51% at 600 °C (not shown).

Figure 2. XRD patterns at room temperature for (A) Cu^{2+}-ion exchanged Al_2O_3-pillared laponite, (B) Cu^{2+}-ion exchanged TiO_2-pillared bentonite, (C) Cu^{2+}-exchanged ZSM-5.

Figure 3. Temperature peak in NO conversion is the result of chemical rate and pore diffusion rate (both increase with T) and hydrocarbon oxidation (to decrease NO conversion at high T). Pore diffusion in macropores in delaminated pillared clay has a higher T dependence than that in micropores in laminated pillared clay, hence resulting in a higher peak temperature for NO conversion.Note curves A and D are also different for the two pillared clays.

Figure 4. FT - IR spectra of ammonia absorption at 25°C on Cu^{2+}-exchanged alumina-pillared laponite followed by helium purge at (A) 25°C, (B) 200°C, (C) 300°C, (D) 350°C, (E) 410°C.

Figure 5. Oxygen effect on SCR activity over Cu^{2+}-ion exchanged Al_2O_3-pillared laponite. Reaction conditions: NO = 1,000 ppm, C_2H_4 = 1,000 ppm, O_2 = 0%-4%, catalyst = 0.5 g, N_2 = balance, total flowrate = 250 cc/min.

Figure 6. Poisoning effect of water and SO2 on the catalyst for SCR of NO by ethylene. Conditiuons: NO = 1000 ppm, C2H4 = 1000 ppm, O_2 = 2%, SO_2 = 500 ppm (when used], H_2O = 5% (when used), N_2 = balance, catalyst = 0.5 g and total flowrate = 250 cc/min.

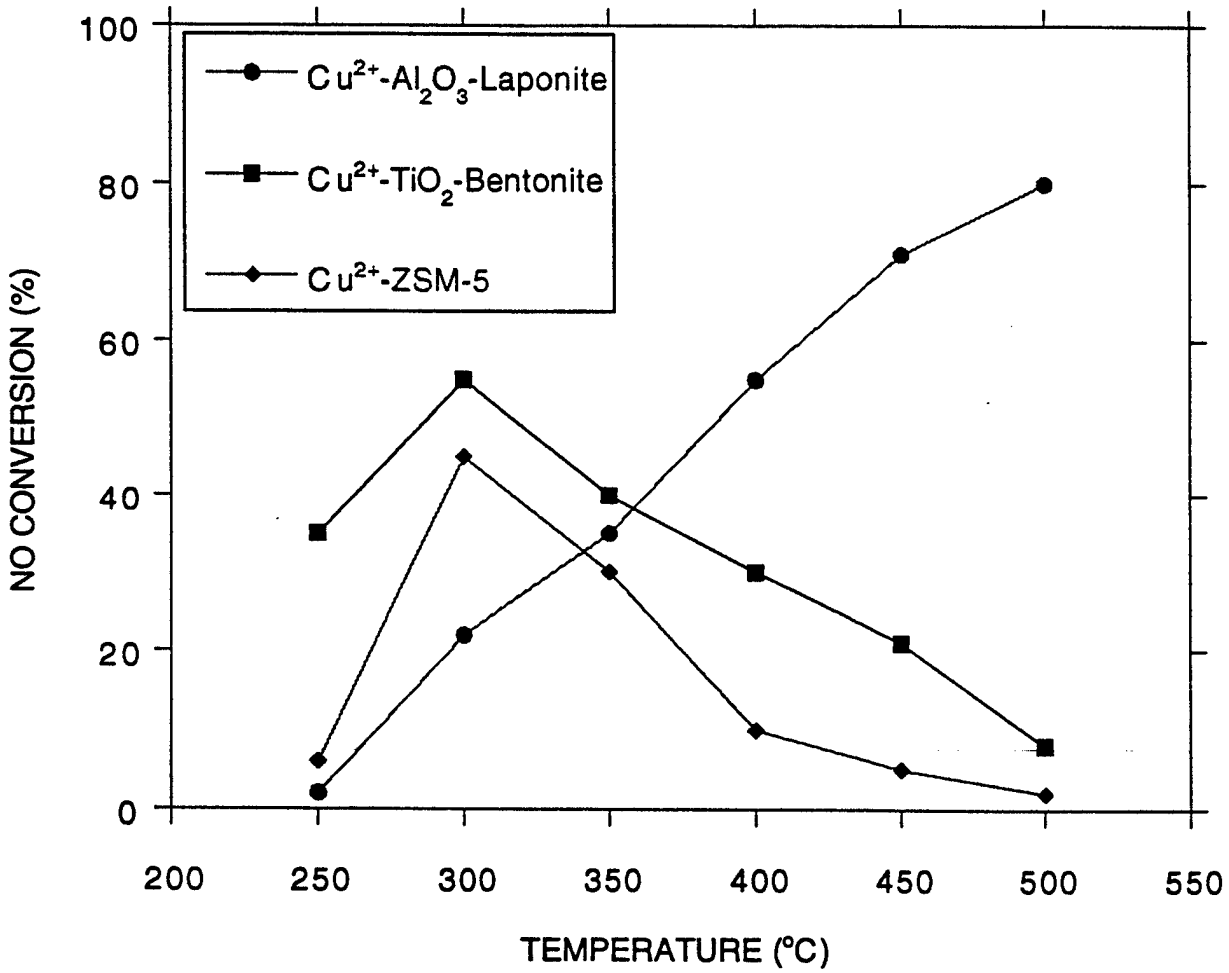
100
80
60
40
20
0
NO CONVERSION (%)
200
250
300
350
400
450
500
550
TEMPERATURE (°C)
Cu2+-Al2O3-Laponite
Cu2+-TiO2-Bentonite
Cu2+-ZSM-5

Fig. 1.

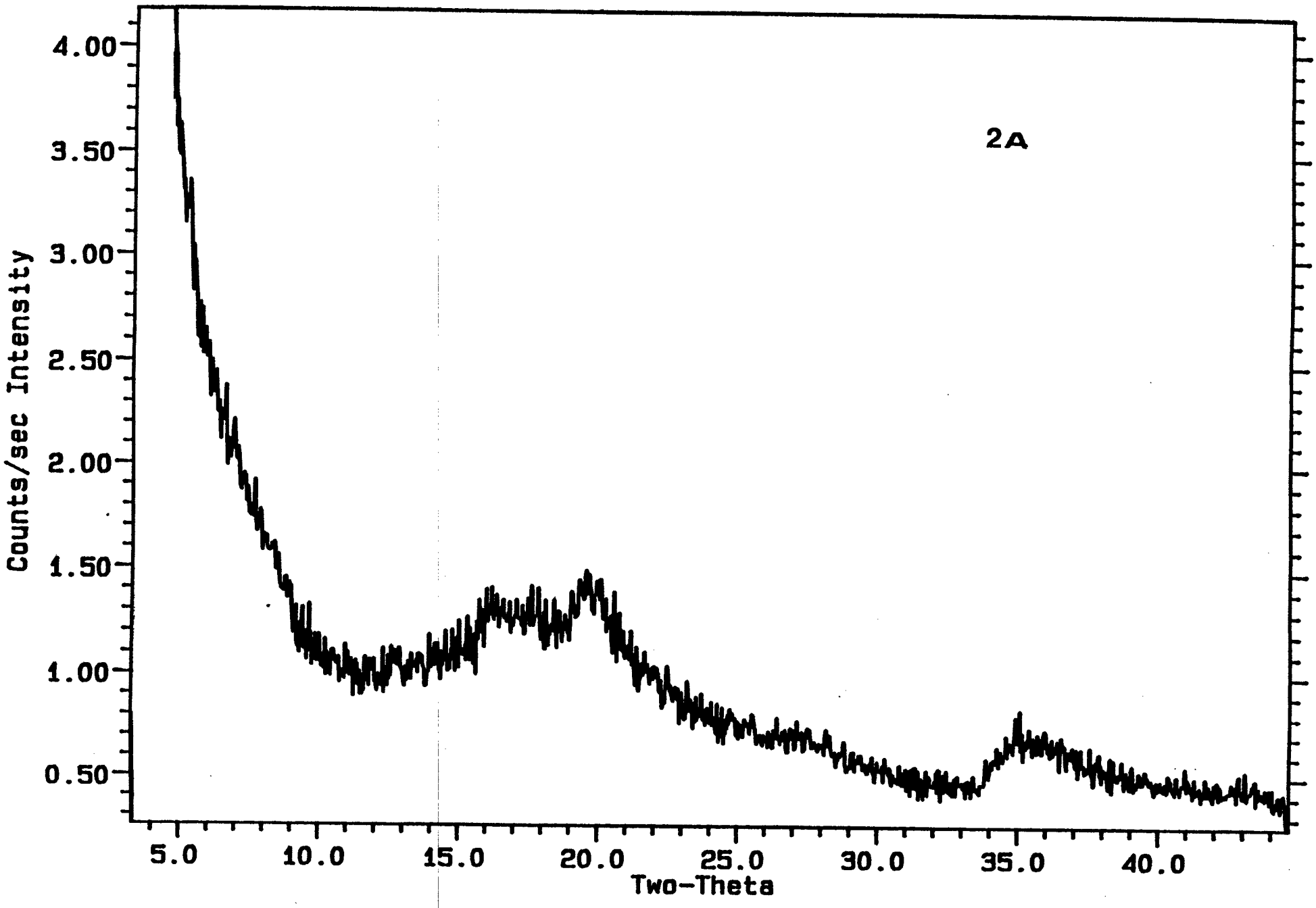
2A
Counts/sec Intensity
4.00
3.50
3.00
2.50
2.00
1.50
1.00
0.50
5.0
10.0
15.0
20.0
25.0
30.0
35.0
40.0
Two-Theta

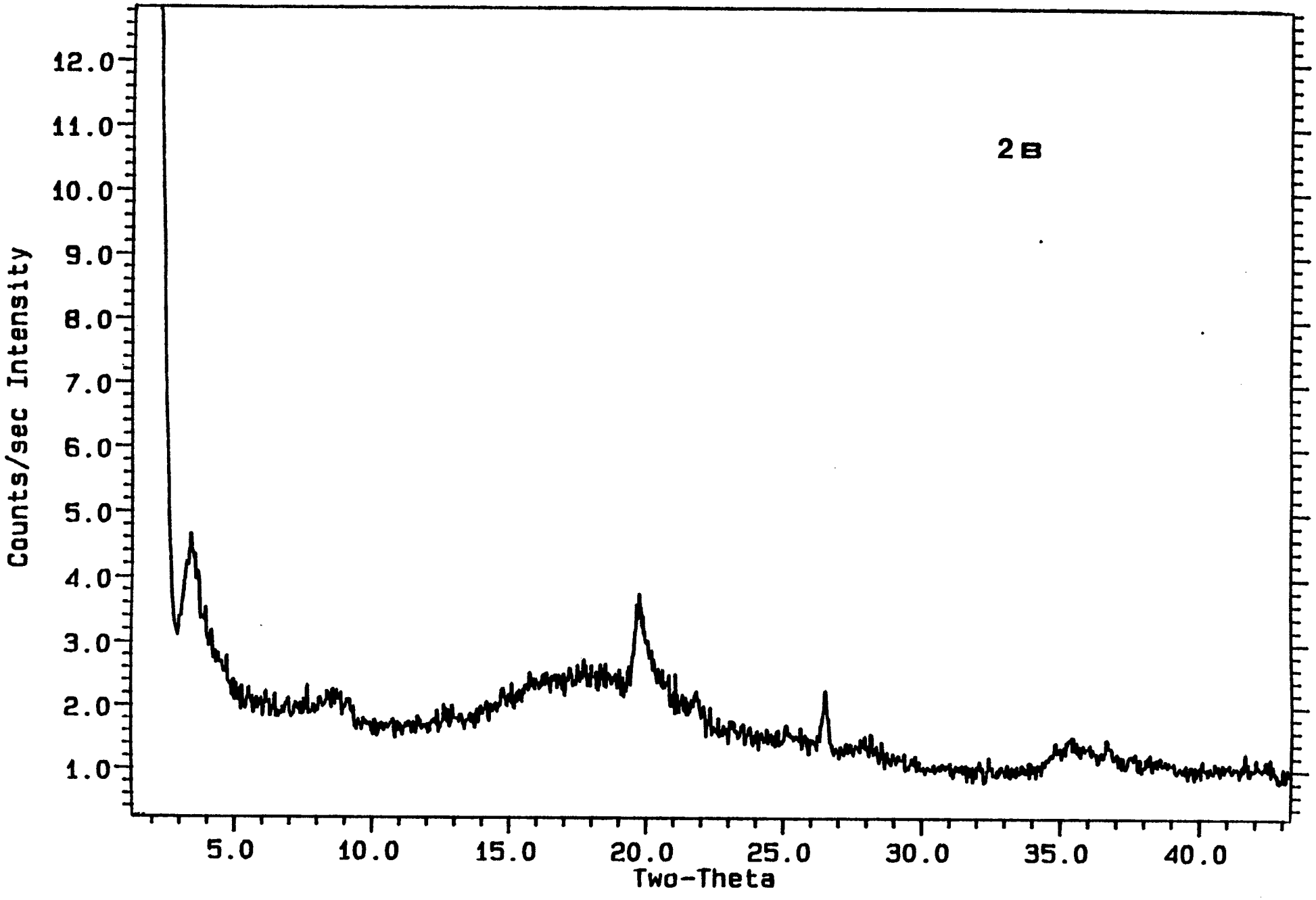
2B
Counts/sec Intensity
12.0
11.0
10.0
9.0
8.0
7.0
6.0
5.0
4.0
3.0
2.0
1.0
5.0
10.0
15.0
20.0
25.0
30.0
35.0
40.0
Two-Theta

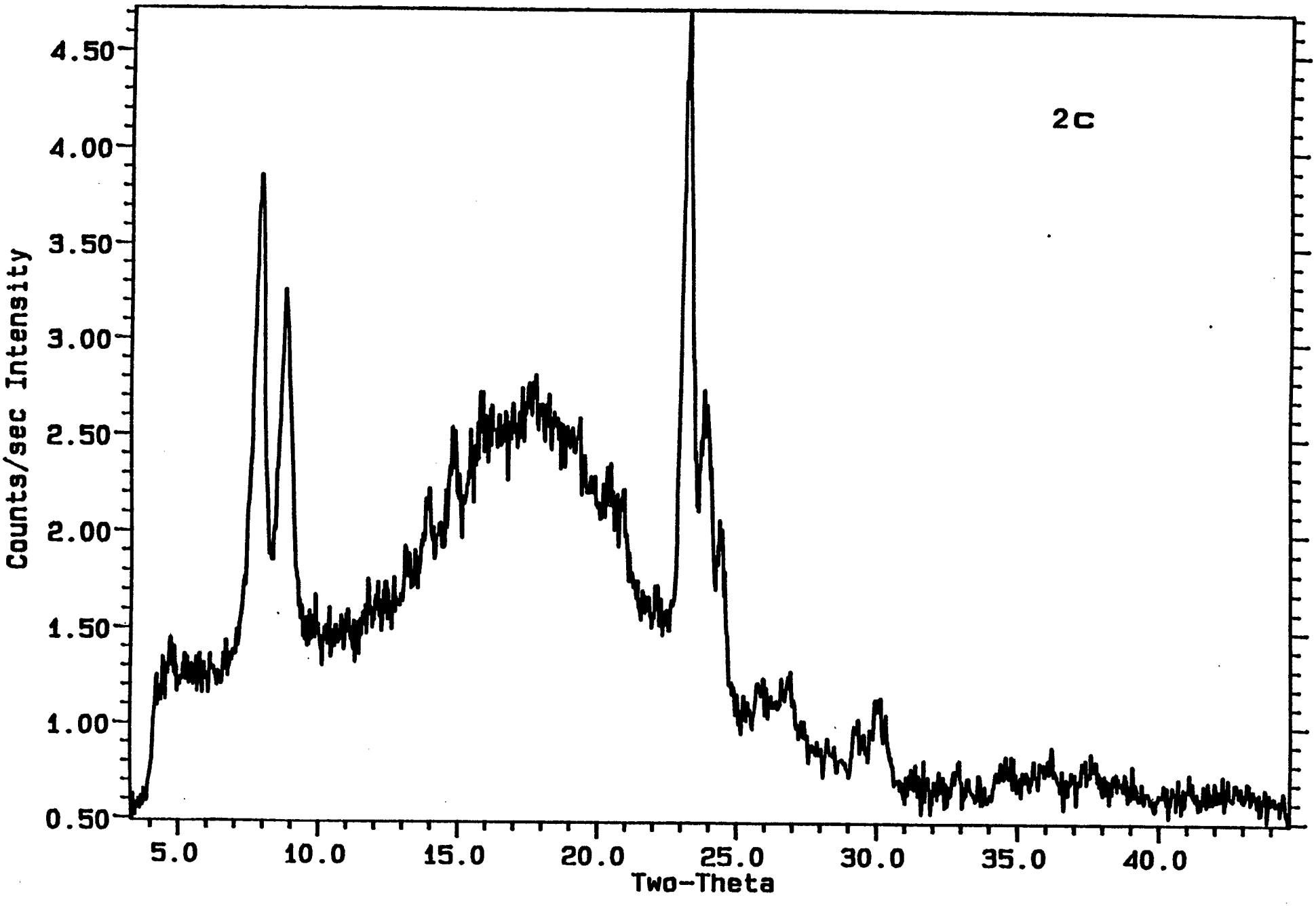
2c
Counts/sec Intensity
4.50
4.00
3.50
3.00
2.50
2.00
1.50
1.00
0.50
5.0
10.0
15.0
20.0
25.0
30.0
35.0
40.0
Two-Theta

Fig 2c

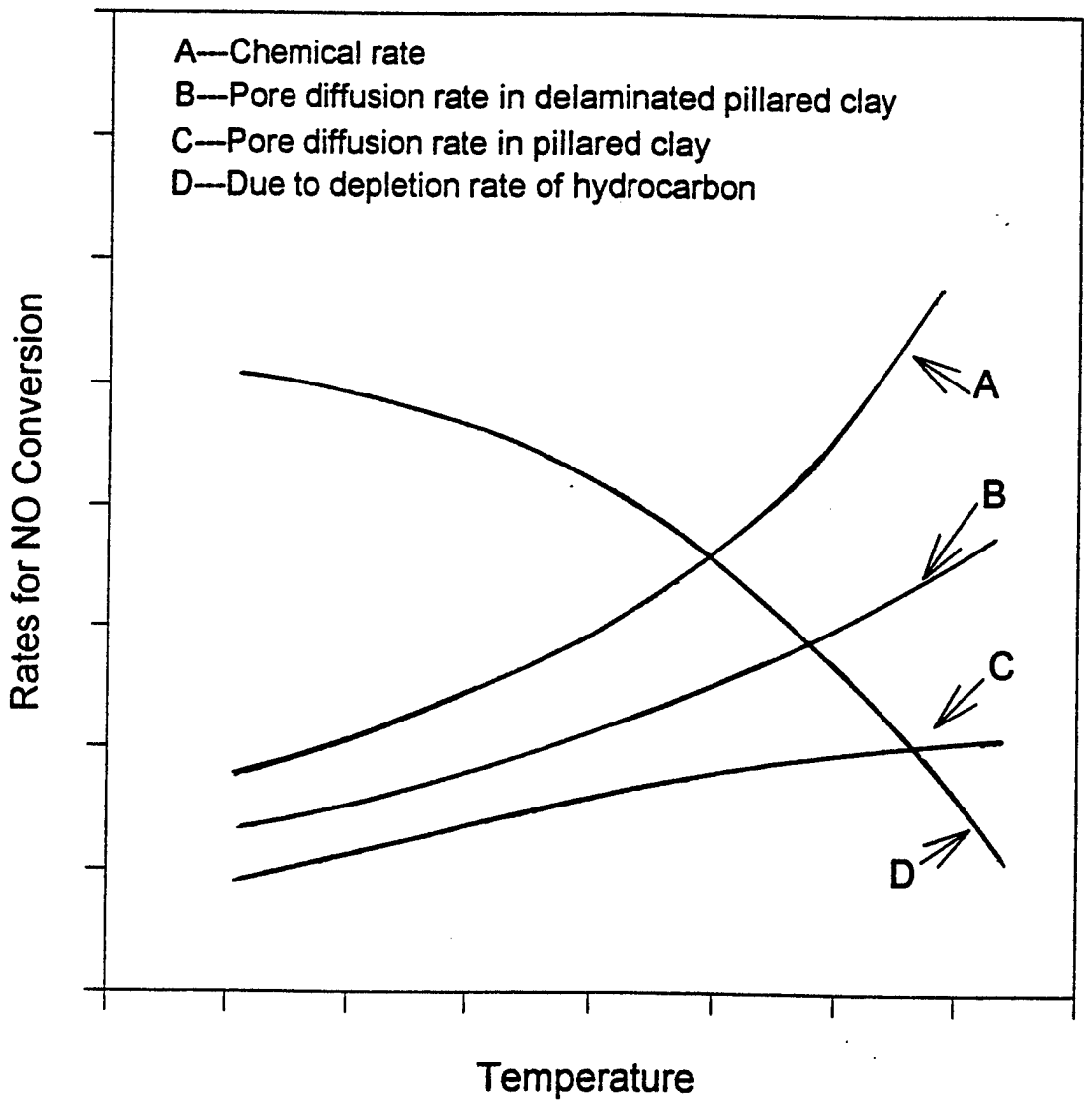
A---Chemical rate
B---Pore diffusion rate in delaminated pillared clay
C---Pore diffusion rate in pillared clay
D---Due to depletion rate of hydrocarbon
A
B
C
D
Rates for NO Conversion
Temperature

Fig. 3

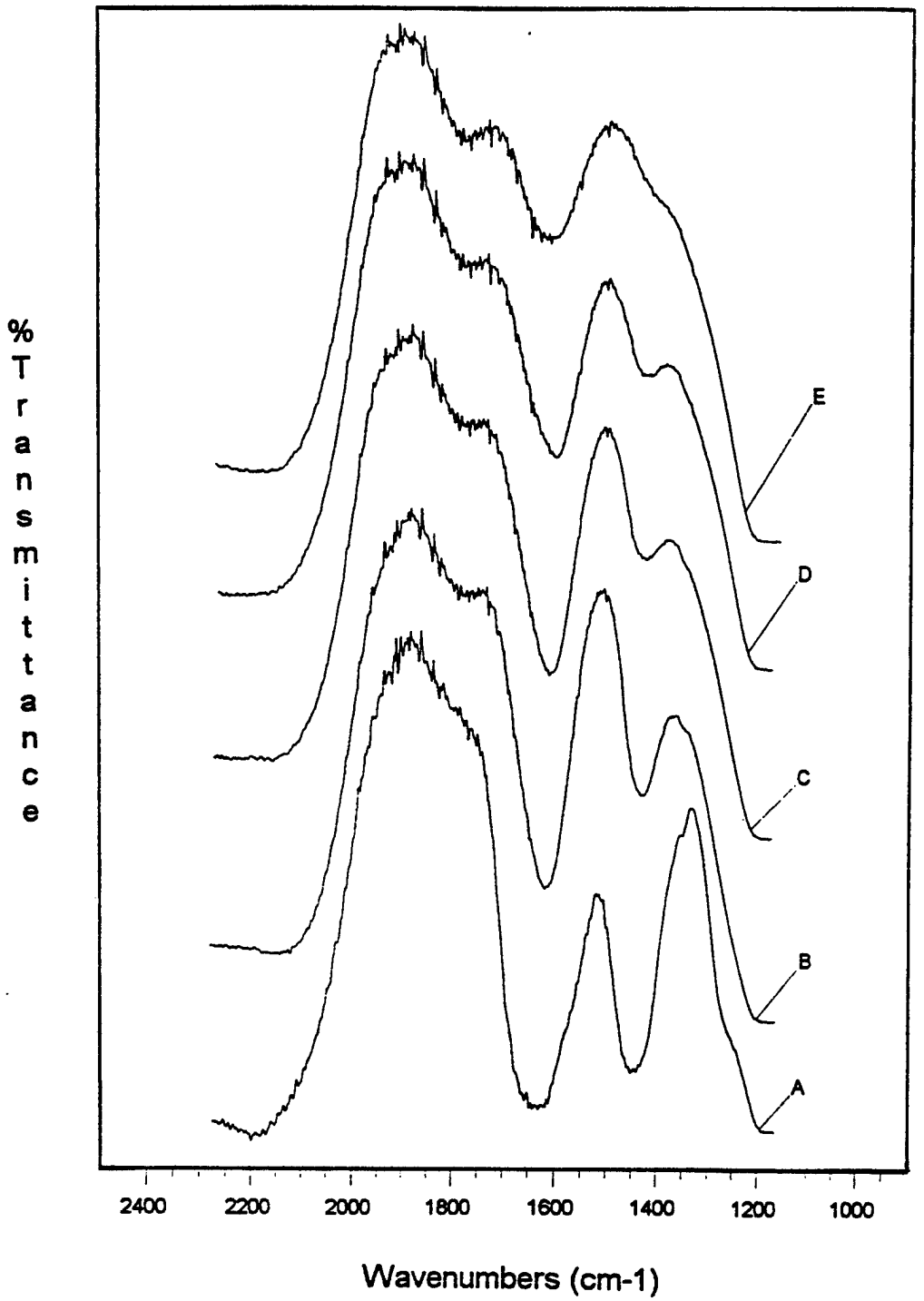
%Transmittance
E
D
C
B
A
2400
2200
2000
1800
1600
1400
1200
1000
Wavenumbers (cm-1)

Fig. 4

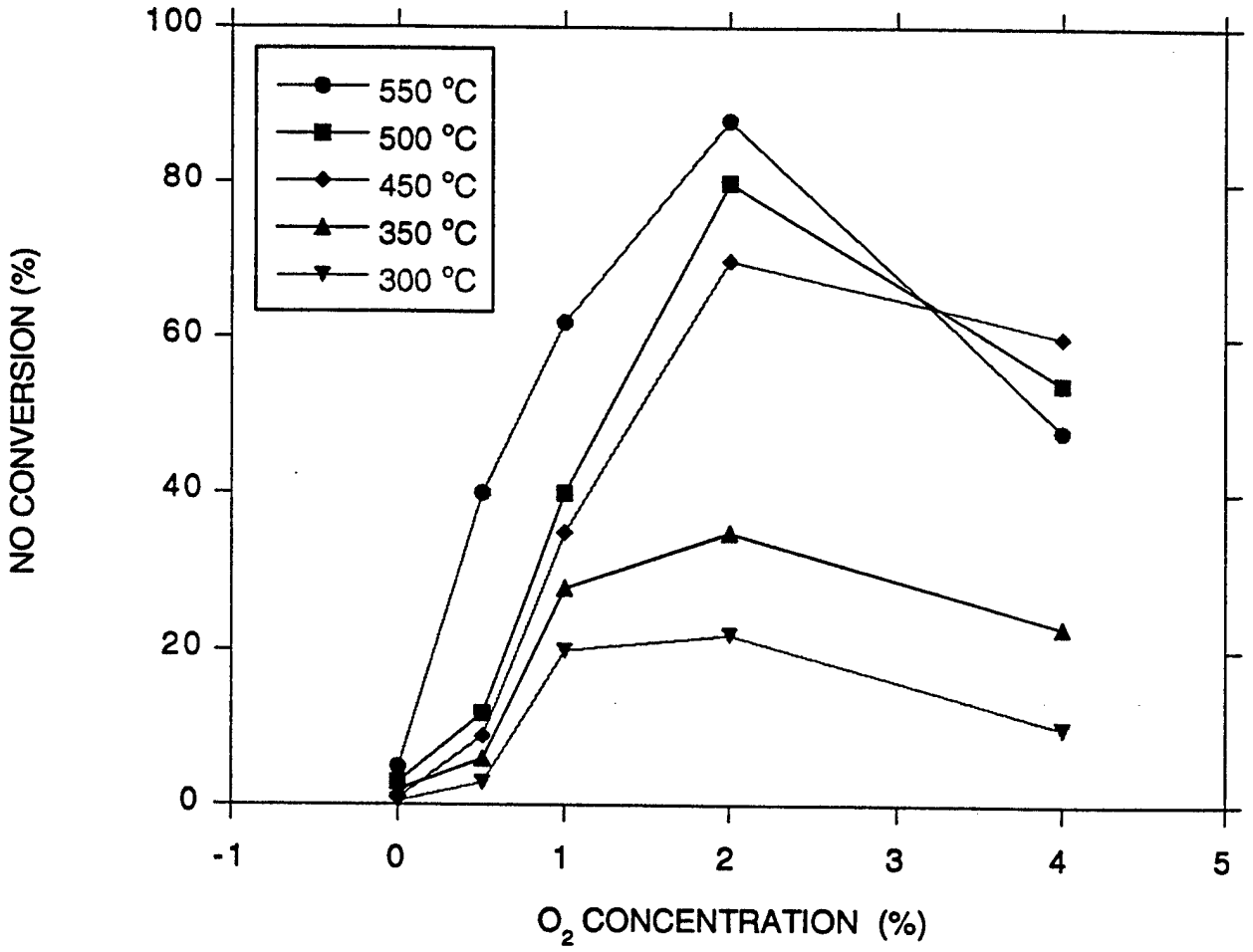
100
80
60
40
20
0
-1
0
1
2
3
4
5
550 °C
500 °C
450 °C
350 °C
300 °C
NO CONVERSION (%)
O2 CONCENTRATION (%)

Fig. 5

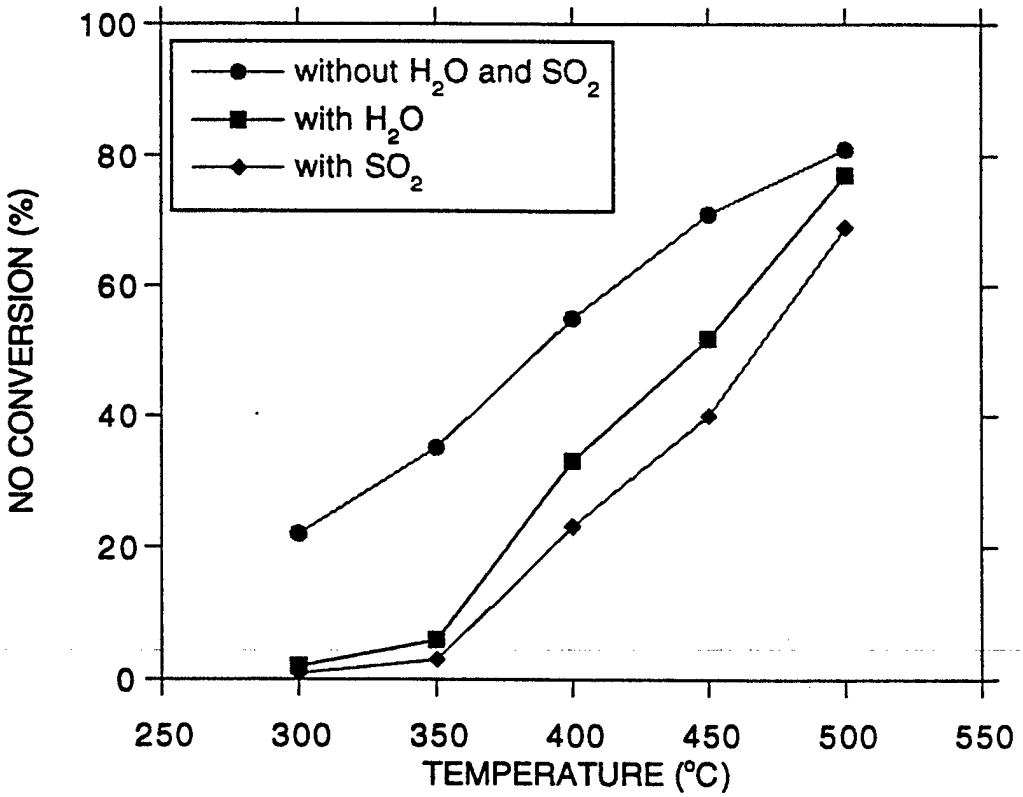
100
80
60
40
20
0
NO CONVERSION (%)
without H_2O and SO_2
with H_2O
with SO_2
250
300
350
400
450
500
550
TEMPERATURE (°C)

Fig. 6

Part Two: Fourier Transform Infrared Spectroscopy Study of the NO Decomposition Mechanism on Cu2+ Ion Exchanged Alumina Pillared Clay

Abstract

In an earlier study, it has been found that Cu^{2+} ion-exchange pillared clay (Cu-PILC) has a substantially higher activity for the selective catalytic reduction of NO by ethylene over Cu-ZSM-5. Moreover, it is not significantly deactivated by water vapor and SO_2. In this study, the activity for direct NO decomposition in the presence of O_2 on Cu-PILC was measured and an in situ IR study for the key intermediates and the reaction mechanism was made. Under in situ NO and O_2 reaction conditions at temperatures up to 300 °C, IR absorption bands at well-defined peak positions are identified. The band at 1699 cm^{-1} is assigned to be dinitrosyl species on Cu^{+}. The bands with peaks at 1609,1530-1480 and in the region of 1440-1335 cm^{-1} are assigned to be bidentate nitrate, monodentate nitrate and nitro species bonded to Cu^{2+}. A redox mechanism is proposed. The limiting step is thought to be the N-N coupling between surface nitrate and gaseous nitric oxide to form nitrogen. The existence of substantial amounts of nitrate formed from NO alone indicates the important role of the large amount of lattice oxygen that is available on Cu-PILC. As a result, the role of external oxygen supply is only to replenish the consumed lattice oxygen. The proposed NO decomposition mechanism suggests that the redox property of Cu-PILC is crucial for this reaction.

Introduction

NO_x catalytic decomposition and reduction have been studied extensively because it is a major concern in air pollution. High NO_x emission from combustion sources emitted to the atmosphere contributes to acid rain and smog formation. More stringent regulations have been imposed recently to lower the pollutant emission of hydrocarbon, carbon oxides, nitric oxides and particulates. All of these pollutants excluding NO_x can be minimized by operating

combustion engines at a high air to fuel ratio, i.e., under lean burn conditions(1). Such highly oxidizing conditions would dramatically diminish the activity of the catalyst used in conventional three way catalytic converters which are used to eliminate HC, CO, and NO_x. The situation becomes worse when the combustion temperature has been raised for higher standards of fuel efficiency (2-5). These changes present a challenge to search for new catalysts or methods to deal with the increased NO concentrations from the lean-burn engines. Thus, many studies have been conducted to search for the best catalysts and alternate approaches which could selectively convert NO_x to nontoxic substances under the real exhaust condition and compositions. Earlier research was focused on NO_x decomposition over noble metal catalysts(6). This method is preferred because no additional chemicals are required to decompose NO_x to N_2 and O_2. Although direct decomposition is thermodynamically favorable, the rates are prohibitively low (7). The first catalysts found to be active for selective catalytic reduction (SCR) of NO by hydrocarbons in the presence of oxygen were Cu^{2+} ion-exchanged ZSM-5 and other zeolites, reported in 1990 by Iwamoto (8) and Held et.al.(9) and in early patents cited in (10). Reports on a large number of catalysts for this reaction have appeared since 1990(11,12). The majority of these catalysts are ion-exchanged zeolites, including H^+ forms. Alumina and metal oxides supported on alumina have also been studied, but are less active. The early (1992-1993) literature on the subject, primarily by Japanese researchers, has been reviewed by Iwamoto and Mizuno(4) and will not be repeated here. The most active catalysts include: Cu-ZSM-5 (7-9,13-19), Co-ZSM-5 and Co-Ferrierite(18,20-22), Ce-ZSM-5(10,23), and Cu-Zr-O and Cu-Ga-O (24,25). Although Cu-ZSM-5 is the most active catalyst, it suffers from severe deactivation in engine tests, presumably due to H_2O and SO_2(26-28). Comprehensive reviews and discussion on the reaction were made recently by Amiridis et al. (12) and by Shelef(29). More recently, Yang and Li(1995) found that Cu^{2+} ion-exchanged pillared clay (PILC) has superior NO SCR activities (using C_2H_4). Based on comparison of first-order rate constants for Cu^{2+} -PILC and Cu^{2+}-ZSM-5, the PILC catalyst was four times more active at 300 °C, and more importantly, the PILC catalyst maintained high activities in the

presence of H_2O and SO_2(Yang and Li,1995). The mechanism of the SCR reaction on Cu^{2+}-PILC is not understood (Li et al.,1996).

This study was designed to obtain an understanding of NO decomposition on Cu^{2+}-PILC as the first step to understand the SCR mechanism. Due to the similarity between Cu^{2+}-PILC and Cu-ZSM-5, the previously proposed mechanisms on Cu-ZSM-5 would provide some insights into the reaction on Cu^{2+}-PILC. For example, Li, Hall and Valyon have suggested that "the working catalysts probably consist of a relatively small number of Cu(I) centers (or adjacent Cu(I) pairs) maintained in a steady state by balance of the rate of oxidation with the rate of O_2 desorption" (30,31). This is consistent with Iwamoto and Hamada (32) who studied the copper oxidation states and examined its influence on the interactions of Cu with adsorbates under various conditions by FTIR,ESR,TPR and techniques. Giamello et al. also explained the redox cycle by N_2O elimination from the dinitrosyl species(5,33). It has been suggested that N_2O_3 was an intermediate species (5,34,35). Therefore, the purpose of this study was to explore the detailed mechanism by using mainly FTIR to study the surface species on Cu^{2+}-PILC under the in situ conditions.

Experimental

a) Cu^{2+}-Ion Exchange and Catalyst Preparation

A delaminated form of pillared clay, delaminated Al_2O_3- pillared laponite, was used in this study. The PILC was prepared by Laporte Industries,Ltd. The sample was pretreated by first suspending as 1% slurry (by weight) and then washing with dilute NH_4NO_3 solution to remove impurities and remaining metal ions. After filtration, the residue was dried at 110 °C in air and resuspended as 1% slurry (by weight). 10 ml. of 0.1M $Cu(NO_3)_2$ solution was added to 100 ml. slurry with constant stirring. The acidity of the solution was controlled to pH=5.5 by using ammonium hydroxide and nitric acid solutions. The mixture was then kept at 50 °C for 6 hr. The residue was then thoroughly washed with de-ionized water 5 times. After filtration, the solid sample was dried at 100 °C for 24 hr., crushed, sieved for the size fraction 80-100 US mesh and calcined at 400 °C in air for 12 hr. The amount of the transition metal ions (Cu^{2+}) in

the PILC was determined by atomic absorption spectroscopy. The catalyst contained 3.9% Cu. From BET analysis, the sample surface areas were 384 m^2/g and 318 m^2/g, respectively, for delaminated alumina-pillared laponite and its Cu^{2+}-exchanged form.

b) FTIR Spectroscopy

A Nicolet-400 spectrometer was used to record the FTIR spectra. The sample was pressed into self-supporting wafers and mounted in a pyrex glass IR cell fitted with CaF_2 windows. The FTIR cell was designed for in situ reaction. A heating element cage surrounding a movable sample holder was employed to heat the catalyst temperature up to 450 °C. The temperature was measured with a chromel-alumel thermocouple mounted close to the catalyst surface. Spectra were taken by accumulating 100 scans at a spectral resolution of 4 cm^{-1} . The focused wavelength range was 3000-900 cm^{-1} to observe the related nitro, nitrile, nitrito and nitrate species. A delaminated Cu^{2+} - Al_2O_3- pillared laponite pellet of about 25 mg/cm^2 was used for this study.

Before recording background or sample spectra, the pellet was pretreated under a flow of UHP He at 400 °C for 2 hr at a flow rate of 100 ml/min. After pretreatment, the background was recorded after the clean pellet remained at the desired temperature for 15 min. to ensure that thermal equilibrium was reached. The background spectra were collected at several temperatures that corresponded to the in situ reaction temperatures. Subsequently, the catalyst was exposed to a stream of NO(0.6%) in He balance (supplied by Matheson company, used without further purification) at a total flow rate of 60 ml/min at room temperature for half an hour. Then, the gases were switched off and the catalyst was purged by He until there was no gas phase species shown in the spectrum. The sample was heated to the desired temperature at 10 °C per min. These spectra were recorded in series from room temperature to 300 °C at 100 °C intervals. In addition, the effects of O_2 gas were also studied. After the foregoing pretreatment, O_2 gas (99% purity) was mixed with the stream of NO (0.6%) and He by maintaining the total flow rate at 60

ml/min. The spectra were taken in two separate sets. One was for room temperature adsorption. The procedure for recording the spectra was the same as stated above for NO. The other was to observe the difference by using a subtraction method under in situ condition as to be descibed. The background was recorded under the reactant gases and then subtracted from the spectra of adsorbed species under those reactant gases at the same concentration.

c) NO Decomposition and Product analysis

Catalyst activity was studied in a fixed bed quartz micro reactor. The catalyst was subjected to the pretreatment under a flow of UHP He at 100 ml/min at 300 °C for 2 hr. Gas flow rates were regulated by volumetric flow controllers. A 10,000 ppm NO balanced with He passed through the 0.35 g sample supported on a quartz frit. The total gas flow rate was 40 cm^3 STP/min. The product stream was analyzed by a chemiluminescent NO/NO_x analyzer (Thermo Electron Corporation, Model 10) and a mass spectrometer (UTI Instrument, model 100). The chemiluminescent NO/NO_x analyzer with a sensitivity of 1 ppm was used for continuously monitoring the product NO concentration. The detailed equipment description was given elsewhere(36). In addition, a Shimadzu GC model 14A gas chromatograph was used to analyze the trace amounts of N_2 and N_2O in the reactor product stream, from 1 cm^3 manual samples. A Poropak Q column was used to analyze NO, N_2O and a molecular sieve 5A column to analyze N_2 and O_2. The temperature of the TCD detector was set at 50 °C for Poropak Q in order to clearly resolve the N_2O peak, and the temperature was set at 25 °C for the molecular sieve column(37). For the mass spectrometric analysis, a Quadrupole Gas Analyzer was used for N_2O analysis.

Results

Figure 1 shows the FTIR spectra at various temperatures after 6,000 ppm NO adsorption at room temperature on Cu^{2+}-Al-PILC. The IR absorption bands of gaseous NO are

at 1900 and 1840 cm^{-1}. These two peaks vanished after purging with He for a short period. The remaining peaks appeared at 1699 cm^{-1}, 1603 cm^{-1} and a region of 1453-1310 cm^{-1}. Upon heating to 100 °C, the substantial peak in the vicinity of 1450-1300 cm^{-1} resolved into two peaks, centered at 1493 and 1334 cm^{-1} while there was no noticeable intensity reduction. In contrast, the intensity of the small shoulder at 1603 cm^{-1} diminished somewhat while the band at 1699 cm^{-1} completely disappeared. Further increasing the temperature to 200 °C, the pair of peaks at 1493 and 1334 cm^{-1} shifted slightly to higher and lower frequencies at 1571 and 1306 cm^{-1}. These two peaks demonstrated thermal stability up to 200 °C and started decreasing their intensity when the temperature was increased to 300 °C. In addition, a pair of gaseous CO_2 peaks between 2380-2300 cm^{-1} was detected due to CO_2 trapped in stagnant areas in the FTIR cell. A set of negative O-H stretching bands was also observed in the region of 3800-3600 cm^{-1} and gradually increased at higher surface temperatures.

Figure 2 shows the FTIR spectra at various temperatures after 6,000 ppm NO and 2% O_2 adsorption at room temperature on Cu^{2+}-Al-PILC, followed by He purge. It clearly shows that the presence of O_2 did not contribute to any additional species when compared to pure NO preadsorption. All peaks were at the same positions as in Figure 1.

Figure 3 shows the FTIR spectra of the adsorbed species at various temperatures in 6,000 ppm NO and 2% O_2 on Cu^{2+}-Al-PILC. These were in situ conditions. Compared to Figure 2, these spectra, under the in situ reaction condition, indicate the significant intensity reduction at high temperatures.

Figure 4 shows the spectra of Cu^{2+} -Al-PILC without exposure to NO and O_2. The spectrum at room temperature shows a broad band at 2900-3750 cm^{-1}, which is the stretching band for hydrogen bonded water adsorbed on the surface plus the hydroxyl groups. As the temperature was increased, water desorbed and this band became sharpened. Sharp bands at

3600 - 3750 cm^{-1} are due to free OH hydroxyl groups on the surface which could remain at temperatures substantially higher than 300°C.

The activity of the catalyst for direct NO decomposition was measured. Product analysis was made to measure the NO conversion and to see if N_2O was formed. At 200 °C, the NO conversion from the NO/NO_x chemiluminescent analyzer was approximately 10% at 1.0 g.s. cm^{-3} for an inlet concentration of 1% NO. This can be compared with 8% NO conversion over Cu-ZSM-5 at 4.0 g.s. cm^{-3}, also at 1% NO(21). A comparison of the SCR activity of NO with C_2H_4 between these two catalysts has already been made(38) and will not be repeated here. With on-line mass spectrometer measurements, we detected small trace amounts of a species at 44 amu which was assigned to be N_2O. Its concentration initially increased and subsequently leveled off. Its concentration history was parallel with that of nitrogen. The N_2O concentration was, however, at a low level such that it was not detectable by the G.C., i.e., well below 1%.

Discussion

Owing to its stability under the He purge over 1 hr, the possibility of assigning the peak at 1699 cm^{-1} to the physisorbed species has been ruled out. This species is thought to be dinitrosyl, disappearing at a temperature greater than 100 °C, and it was bonded to Cu^+. It was reported that both mononitrosyl and dinitrosyl species were formed on Cu^+ sites, whereas mononitrosyl formed exclusively on Cu^{2+} ions(33,39,40). The small shift from the band positions on Cu-ZSM-5 as assigned by Valyon and Hall (1827,1734 cm^{-1})(41) is possibly due to stronger coordination between the metal site and nitric oxide. The acceptance of an electron transferred from NO to a metal site is more favorable on Cu-PILC and thus, the bond strength of NO becomes weaker when compared to that on Cu-ZSM-5. The peak of symmetric stretching of dinitrosyl is not clearly shown. It might have been disguised by the broad band at 1699 cm^{-1}. Unlike the first peak, the shoulder at 1603 cm^{-1} demonstrates its thermal stability up to 300 °C. It can be possibly assigned as NO_2-containing species (bands at 1630,1608,1574 and 1315

cm^{-1}) as in (35,40,42-43). Nevertheless, due to its robustness which is not likely to be seen in nitro species, this species is more likely a nitrate species. Although the precise structures of these nitro and nitrate species are difficult to assign, many literature sources suggest that the structure is likely of the form bidentate nitrate(34,42,43). The pair of bands at 1603 and 1300 cm^{-1} can be attributed to ν_3 split vibration of either bridge nitrate ($\Delta\nu_3 \approx 420$ cm^{-1}) or bidentate nitrate ($\Delta\nu_3 \approx 300$ cm^{-1}). However, $\Delta\nu_3$ of this species is closer to that of the bidentate nitrate. Also, a bridged nitrate would require two coupled sites to form, which is not a likely event. Therefore, this species is assigned to be bidentate. The bidentate ν_1 vibration frequency at 1040-1010 cm^{-1} could not be detected in this experiment. The remaining broad band is suspected to contain at least two species. They apparently split and drift apart at higher temperatures. The regions of 1440-1335 cm^{-1} and 1385-1250 cm^{-1} have been assigned to be $\nu_3(NO_2)$ (ν_3 = 1470-1450 cm^{-1}) and $\nu_1(NO_2)$ (ν_1 =1065-1050 cm^{-1}) (42,43).

The NO_2 species has been attributed to be a key intermediate species on copper-on-alumina(44). Most of the surface species belong to either nitro species for Cu-ZSM-5 or nitrito for Co-ZSM-5(45). As the precise nature of the nitro, nitrito and nitrato species is not known, the bands in the region of 1530-1630 cm^{-1} and near 1300 cm^{-1} have been unspecifically assigned to all these species(41). As a result, the active nitro species is assigned to be bidentate nitro or nitrito species. When the catalyst is further heated to 200 °C, these two bands drifted further apart to the new positions at 1571, 1306 cm^{-1}.The peak positions at 1571 and 1306 cm^{-1} conform to that of the monodentate nitrate (NO_3^-) in the range of 1530-1480 cm^{-1} for ν_3(split) as noted in (42,43). Its characteristic is consistent with that found by Bell and coworkers as the intensity grew from room temperature and then reduced at 300 °C(34). This assignment is plausible when comparing the monodentate nitrate with relatively low thermal stability and the adjacent peak of the bidentate nitrate(42).

From the spectra, two possible routes to form nitrate are suggested. One is formed directly from the dinitrosyl group, and the other is formed by reacting with the O-H groups. The first route can be explained as follows. At 100 °C, the dinitrosyl species is unstable and rapidly decomposes to N_2O, while oxidizing the metal site to $Cu^{2+}O^-$. The N_2O species must be significantly active as it could not be detected by FTIR (N_2O ~ 2220-2250 cm^{-1}). It is reported that N_2O decomposes to form N_2 on Cu-ZSM-5 more rapidly than NO because of its self-containing N_2 species which therefore requires only a single site(14). The association of active monodentate nitrito or bidentate nitro (peak region of 1440-1335 cm^{-1} and 1385-1250 cm^{-1}) with the available lattice oxygen eventually form monodentate nitrate (NO_3^-). The other possibility is seen from the noticeably negative O-H stretching peaks at near 3700 cm^{-1}. These negative bands that the nitro group ,either from the gas phase or the adsorbed species, react with the hydroxyl group, thus forming nitrate as on TiO_2 at 150 °C(42). (2Cu-OH + 3 NO_2 -----> 2Cu-NO_3 + H_2O + NO) The slightly negative peaks of O-H stretching at room temperature might be caused by the bidentate nitrate formation. The negative O-H stretching signal is attributed to the depletion of O-H bonds with Cu sites while water as a reaction product desorbs upon He purge or temperature increase. The increasing negative signal is due to more favorable condition for nitrate formation at higher temperature. However, Bell and coworkers have proposed another route by having NO approaching Cu^{2+} sites instead, and subsequently forms a bidentate nitro species on Cu-ZSM-5(34), and consequently generating N_2O_3 (~1600 cm^{-1}) via a Eley-Rideal type reaction of NO and the adsorbed bidentate nitrate(34,46). However, the spectra result in Fig.1 clearly indicates that there are no peaks of these species and thus, confirming that PILC has a different pathway to decompose NO. The proposed mechanism is summarized below.

Proposed mechanism

$2Cu(OH)^+ \longleftrightarrow 2Cu^+ + 1/2\ O_2 + H_2O$ (1)

$Cu^+ + 2NO \longleftrightarrow Cu^+(NO)_2$ (2)

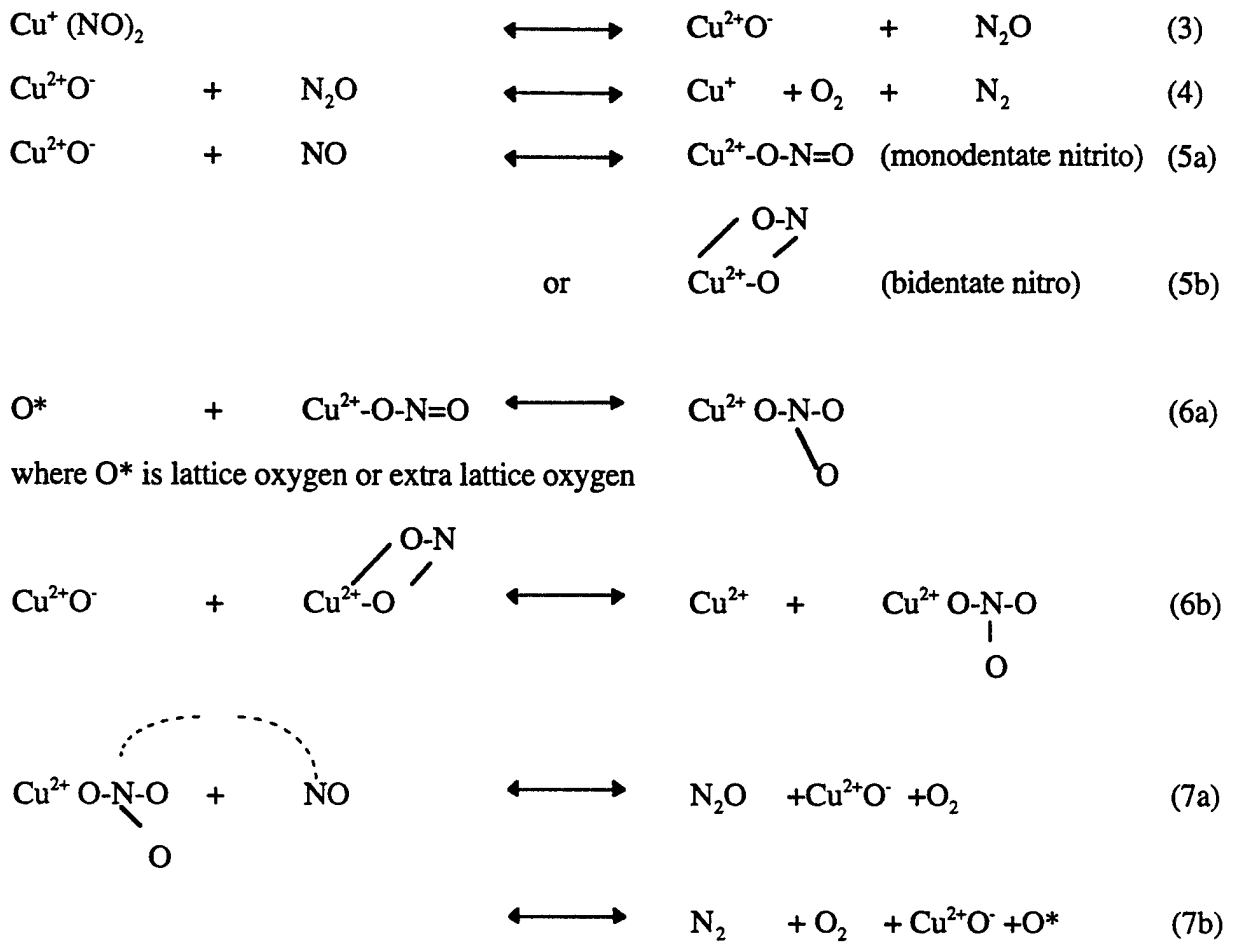

The above mechanism favors the redox cycle on the active sites. The initial occurrence of Cu^{+} could be generated from slightly reduced condition. Water molecules which are coordinated near Cu^{2+} ions are easily ionized and dissociated, and subsequently $Cu(OH)^{+}$ and Bronsted acid sites are formed as observed on Cu-MFI-116 zeolite(47). Some lattice oxygen atoms are probably held by bridge structure of Cu^{2+} -O- Cu^{2+} from dehydroxylating the dimerization or polymerization of $CuOH^{+}$ on a fresh catalyst (41,47). The appearance of Cu^{+} is thus formed from the reduction of Cu^{2+} by 1/2 O_2 evolution(48). The steps are summarized below,as in (50):

Another possibility for Cu^+ formation is from the spontaneous desorption of O_2. Some cupric moieties migrate on the surface of the mesopores and thus the formation of a transient dicopper species generates cuprous ions through the desorption of O_2 (7). Although O_2 coupling especially in the bridge structure, which requires four cations, is quite rare as the metal sites are far apart, there is evidence for spontaneous oxygen desorption on Cu-zeolites even at low temperatures, e.g. room temperature(46). The role of the Cu^+ species is to trigger the aforementioned mechanism. After the cycle is initiated, Cu^+ can be subsequently generated from other intermediates as shown in step 4 through N_2O decomposition. In all, the decomposition of NO to $N_2 + O_{ads}$ at elevated temperatures will lead to reoxidation of Cu^+ to Cu^{2+} and reduce back to Cu^+ under a steady supply of nitric oxide. This result is consistent with the findings of Iwamoto and Hamada(32) and of Hall and co-workers(30,31). However, Shelef argued that there is no cyclical reaction for NO decomposition. His observation is based on the requirement that the adsorption sites remain stable during reaction conditions and be resistant to chemisorption of oxygen(11). He suggests gem-nitrosyl (two NO^- on one site) on Cu^{2+} to be a key intermediate species for direct NO decomposition on Cu-ZSM-5. Further study by EPR of copper on PILC, both after adsorption and desorption of oxygen, seems desirable in order to elucidate the nature of these sites.

The role of N_2O is tentatively identified to be either as an initiator for the cyclic mechanism or a product from the parallel reactions(44). Its instability and rapid direct decomposition over Cu-ZSM-5/Cu-Y zeolite(48) indicates that N_2O might be a key intermediate species for the direct NO decomposition. Due to its paired-nitrogen structure, the decomposition of N_2O is an unimolecular reaction, in contrast to NO decomposition that requires pairing of two nitrogen-containing species. The mass spectrometry result shows the parallel concentration trend of N_2O with N_2 formation. This result is in contrast to the cyclic mechanism in which

N_2O forms initially during the formation of the active sites and then decreases(44). For this reason, N_2O might be generated from the decomposition of another intermediate species which is proposed to be nitrate for Cu-PILC, while N_2O is thought to be generated from copper-nitrite-mononitrosyl for Cu-on-alumina catalyst(44). However, the rate determining step for NO decomposition, following a Langmuir-Hinshelwood type mechanism, involves a surface reaction between two adsorbed NO molecules(51). So, the presence of intermediate N_2O enhances the overall NO conversion.

The rate limiting step for direct NO decomposition has long been described to be the nitrogen-pairing step. The conventional Langmuir-Hinshelwood model of pairing two adsorbed species yields the consistent result with the kinetic study of most transition metals on alumina and on quartz for direct NO decomposition(6). However, the probability of pairing two adjacent sites is not high. Hence an Eley-Rideal type reaction between NO and a surface nitrite-mononitrosyl species (N_2O_3) has been proposed recently for Cu-ZSM-5 and Cu-alumina (34,38,49,50, 51). The result from our FTIR study clearly indicates that there are no peaks of Cu- N_2O_3 in the region of 1600 cm^{-1} for NO_2 bidentate and 1900 cm^{-1} for NO stretching as presented in (45,52). As can be seen in Figs.2 and 3, the decreased amount of monodentate nitrate from 200 °C to 300 °C under the reactant gases is much more appreciable in Fig.3 than in Fig.2. In the presence of O_2 , the NO_3^- peak should have increased by oxidizing the nitro species. Thus, its decrease is possibly from being reduced by NO in the gas phase, generating either N_2O or N_2 as shown in step 7. The N-N bond could not be detected from this experiment. This is possibly due to the short life of this intermediate species. However, Hierl et al. reported that nitrate simply decomposed back to NO and O_2 at higher temperatures from their thermodesorption study on $CuO\text{-}Al_2O_3$ (53). Thus, a further study on the role of nitrate would shed light on this argument.

To study the effect of O_2 , Fig.2 has been recorded after adsorbing both NO and O_2 for half an hour. There are no new emerging peaks or any changes in intensities due to the addition of O_2 . This observation clearly explains the role of ELO which could form the intermediate

species without external O_2 supply. As can be seen when comparing Fig.1 and Fig.2, there is no significant influence from the additional O_2 when it is adsorbed at room temperature. Further product analysis needs to be made in order to determine any possible role of O_2. There is a possibility that for the fresh catalyst, the mechanism path follows step(7b) rather than step(7a). The total lattice oxygen is then preserved and thus adding the external oxygen supply has insignificant effect. When the catalyst is aged, an O_2 dose might help recovering the activity; the mechanism path would shift to step(7a) and consequently deplete the lattice oxygen. Eventually the external O_2 source is required to replenish the consumed amount. In contrast, the effect of supplying O_2 from external source or retaining O_2 from NO decomposition product can be negative if the active site is not selective for NO adsorption and reaction, as found on noble metal catalysts(54).

Conclusion

A reaction path for NO decomposition on Cu-PILC has been proposed, which is different from that on Cu-ZSM-5. The active intermediates under the in situ reaction conditions are assigned to be nitro, nitrous oxide and nitrate. In this mechanism, N_2 can be generated from nitrate or nitrous oxide decomposition. It is likely that the reaction in step(5) occurs so rapidly that it is not possible to detect the short-life Cu- N_2O species by FTIR. However, the missing information can be obtained from results from GC and Mass Spectrometry. From this study, Cu-PILC contains a tremendous reservoir of available lattice oxygen on a fresh catalyst. Consequently, adding the external O_2 supply has no significant effect. The proposed reaction is based on the cyclic redox mechanism and a Eley-Rideal type reaction model. However, further study on product analysis would help in a more detailed understanding of the mechanism.

Acknowledgment

This work was supported by the US Department of Energy under Grant DE-FG22-95PC95213.

References

(1) K.C. Taylor, in "Catalysis: Science and Technology," (J.R. Anderson and M. Boudart, Ed.) Vol 5, Springer-Verlag, Berlin (1984).

(2) T.J Truex, R.A. Searles, D.C Sun, Platinum Metals Rev., 36 (1992), 2.

(3) J. Haggin, Pacifichem'95 Honolulu, C&E News, Am. Chem. Soc., Washington, D.C.,Jan 8,1996.

(4) M. Iwamoto, N. Mizuno, J. of Auto. Engineering(1993), 207.

(5) G.P.Ansell,A.F.Diwell,S.E.Golunski,J.W.Hayes,R.R.Rajaram,T.J.Treux,A.P.Walker, Applied Catalysis B:Environmental,2(1993)81-100.

(6) J.W. Hightower, D.A. Van Leirburg. in "The Catalytic Chemistry of Nitrogen Oxides," (R.L. Klimisch and J.G. Larson, Ed.), Plenum, New York, 1975, pp. 63-94.

(7) D. Lin and H. J.Robota, Appl. Catal. B4(1994),155.

(8) M. Iwamoto, "Symposium on Catalytic Technology for Removal of Nitrogen Oxides," pp. 17-22, Catal. Soc. Japan(1990)

(9) W. Held, A. Konig, T. Richter and L. Puppe, SAE Paper900(1990), 469

(10) C. Yokoyama, M. Mizuno, J. Catal., 150(1994),9.

(11) M.Shelef,Catal.Lett. 15(1992),305.

(12) M.D.Amiridis,T.Zhang and R.J. Farrauto, Applied Catalysis B,10(1996),203.

(13) B.K. Cho, J.Catal.142(1993),418.

(14) J. Valyon and W.K. Hall., J Catal.143(1993),520.

(15) J. Petunchi, G. Sill and W.K. Hall, Appl. Catal., B2(1993),303.

(16) A.P. Ansell, A.F. Diwell, S.E. Colunski, J.W. Hayes, R.R. Rajaran, T.J. Truex and A.P. Walker., Appl.Catal.B2(1993),101.

(17) C.H. Bartholomew, R. Gopalakrishnan, P.R. Stanford, J.E. Davison, W.C. Hecker, Appl.Catal., B2(1993),183.

(18) Y. Li and J.N. Armor, Appl. Catal., B3(1992), L31

(19) Z. Chajar,M. Primet, H. Praliaud, M.Chevrier, C. Gauthier and F. Mathis, Appl. Catal. B4(1994),199.

(20) F. Witzel, G.A. Sill, W.K. Hall, J. Catal.149(1994),229.

(21) Y. Li and J.N. Armor, J. Catal. 150(1994),376.

(22) Y. Li, T.L. Slaget and J.N. Armor, J Catal. 150(1994),388.

(23) M. Misono, K.Kondo, Chem. Lett. (1991)1001.

(24) K.A. Bethke, D.Alt, M.C. Kung, Catal. Lett.25(1994),37.

(25) M. Kung, K. Bethke, D. Alt, B. Yang, H. Kung, in " No_x Reduction," (U.S. Ozkan, S. Agarwal and C. Marcelin, Eds.), Chap. XX, ACS Symp. Ser., ACS Washington, DC, 1995.

(26) M.J. Heimrich, M.L. Deviney, SAE Paper 930(1994), 736.

(27) D.R. Monroe, C.L. Dimaggio, D.D. Beck and F.A. Matekunas, SAE Papar SP-930(1994),737.

(28) J.N. Armor, Appl. Catal. B4(1994), N18.

(29) M. Shelef, Chem. Rev.,95(1995), 209.

(30) Y. Li, W.K.Hall, J.Catal. 129(1991),202.

(31) W.K. Hall, J. Valyon, Catal. Lett. 15(1992),311.

(32) M.Iwamoto, H.Hamada, Catal.Today 10(1991),57.

(33) E.Giamello, D.Murphy, G.Magnacca, C.Morterra,Y.Shioya,T.Nomura,M.Anpo, J. Catal., 136(1992),510.

(34) A.W. Aylor, S.C. Larsen,J.A.Reimer, A.T.Bell, J. Catal., 157(1995),592.

(35)K.Hadjiivanov,D.Klissurski,G.Ramis,G.Busca,AppliedCatal.,B:Environmental, 17(1996)251.

(36) R.T.Yang, J.P.Chen, E.S. Kikkinides, L.S. Cheng, and J.E.Cichanowicz, Ind. Eng. Chem. Res., 31(1992),144.

(37) Y. Li, J. N. Armor, Applied Catalysis B: Environmentals(1995),L257-L270.

(38) W.Li, M.Sirilumpen, R.T. Yang, Applied Catalysis B: Environmental (1996), in press.

(39) M.Iwamoto,H.Furukawa,S.Kagawa. Stud.Surf.Sci.Catal.28(1986)943.

(40) G.Spoto,S.Bordiga,D.Scarano,A.Zecchina, Catal.Lett.,13(1992)39.

(41) J. Valyon, W.K. Hall, J Phys. Chem. 97(1993),1204-1212.

(42) K. Hadjiivanov, V. Busher, M. Kantcheva, D. Kliissurski, Langmuir10 (1994),464-471.

(43) A.A. Davydov, IR spectroscopy Applied to Surface Chemistry of Oxides; Nauka: Novosibirsk, 1984.

(44) G.Centi,S.Perathoner,J. Catal.,152(1995),93.

(45) B.J. Adelman,T.Bentel,G.-D. Lei,W.M.H. Sachtler, J. Catal., 158(1996),327.

(46) T.Cheung,S.K.Bhargava,M.Hobday,K.Goger. J. Catal., 158(1996),301.

(47) M.Iwamoto,H.Yashiro,K.Tanda,N.Mizuno,Y.Mine,S.Kagaw, J. Phys. Chem., 95(1991),3727.

(48) M.Iwamoto,K.Maruyama,N.Yamazoe,T.Seiyama, J. Phys. Chem.81(1987),622.

(49) P.A.Jacobs,H.K.Beyer, J.Phys.Chem., 83(1979),1174.

(50) J.O.Petunchi,G.Marcelin,W.K. Hall, J. Phys. Chem.,96(1992),9967.

(51) M.A. Vannice,A.B. Walters, X.Chang, J. Catal.,159(1996),119.

(52) J. Szanyi, M.T. Paffett, J. Catal.,164(1996),232.

(53) R.Hierl, H.P.Urbach,H.Knozinger,J. Chem.Soc.Faraday Trans.,1992,88(3)355.

(54) R.Burch, P.J.Millington, A.P.Walker, Applied Catalysis B:Environmental 4(1994)65.

(55) M.L. Hair, "Infrared Spectroscopy in Surface Chemistry," Marcel Dekker, New York, 1967.

Figure captions:

Figure1 Spectra of adsorbed species on Cu-PILC after NO (6,000 ppm) adsorption for 0.5 hr. and following by He purge at 25 °C (A), 100 °C (B), 200 °C (C) and 300 °C (D).

Figure2 Spectra of adsorbed species on Cu-PILC after NO (6,000 ppm) and O_2 (6%) adsorption for 0.5 hr. and following by He purge at 25 °C (A), 100 °C (B), 200 °C (C) and 300 °C (D).

Figure3 Spectra of adsorbed species on Cu-PILC under NO (6,000 ppm) and O_2 (6%), without He purge, at 25 °C (A), 100 °C (B), 200 °C (C) and 300 °C (D). The spectra were obtained by subtracting spectra without sample pellet from that with sample pellet, at the same temperatures.

Figure4 Spectra of clean Cu-PILC showing O-H stretching frequencies (including hydrogen bonded, adsorbed water at 3000 - 3500 cm^{-1} and free surface hydroxyl groups at 3650 -3750 cm^{-1}), taken at 25 °C (A) and 300 °C (B).

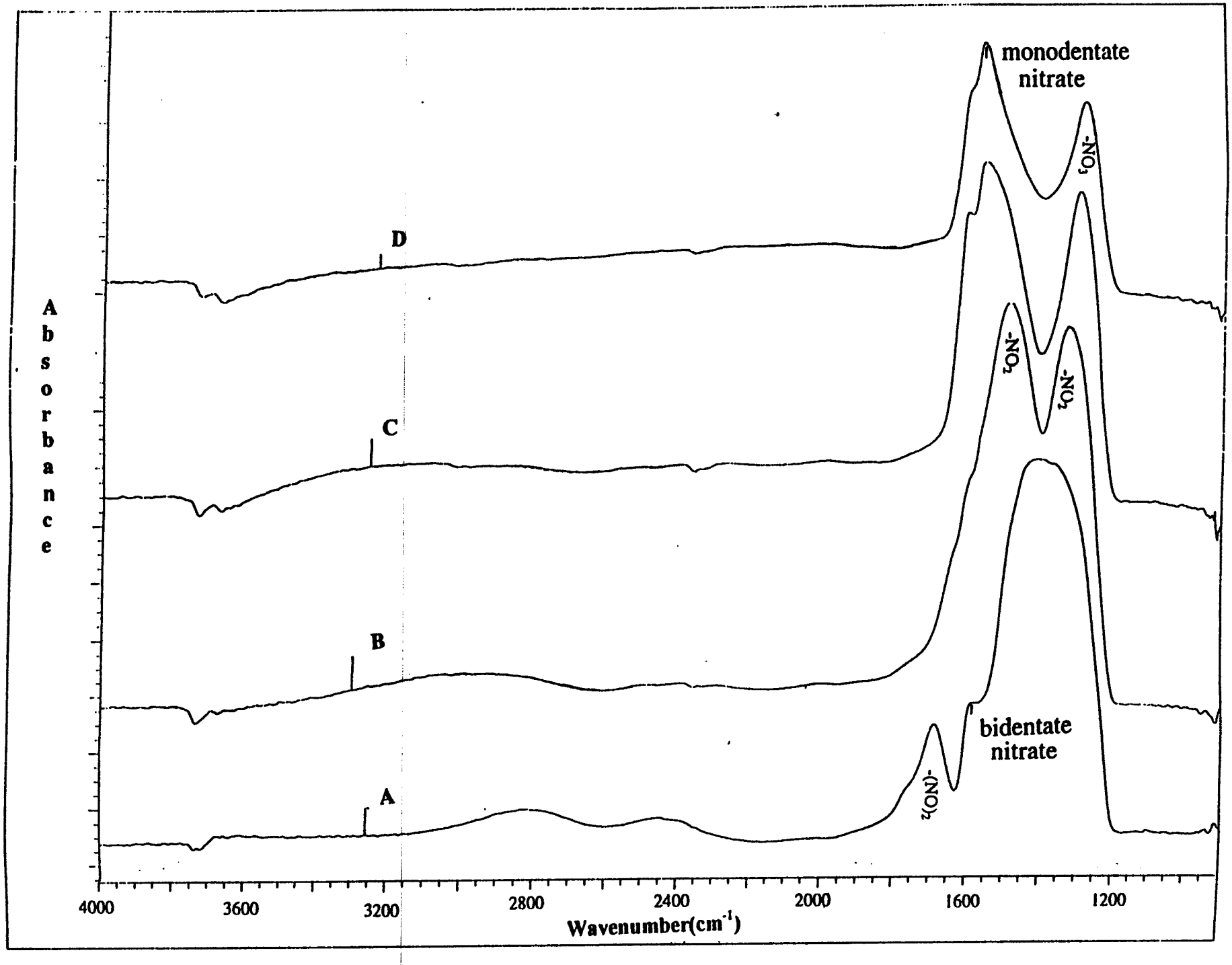
monodentate
nitrate
bidentate
nitrate
D
C
B
A
Absorbance
4000
3600
3200
2800
2400
2000
1600
1200
Wavenumber(cm-1)

Figure 1

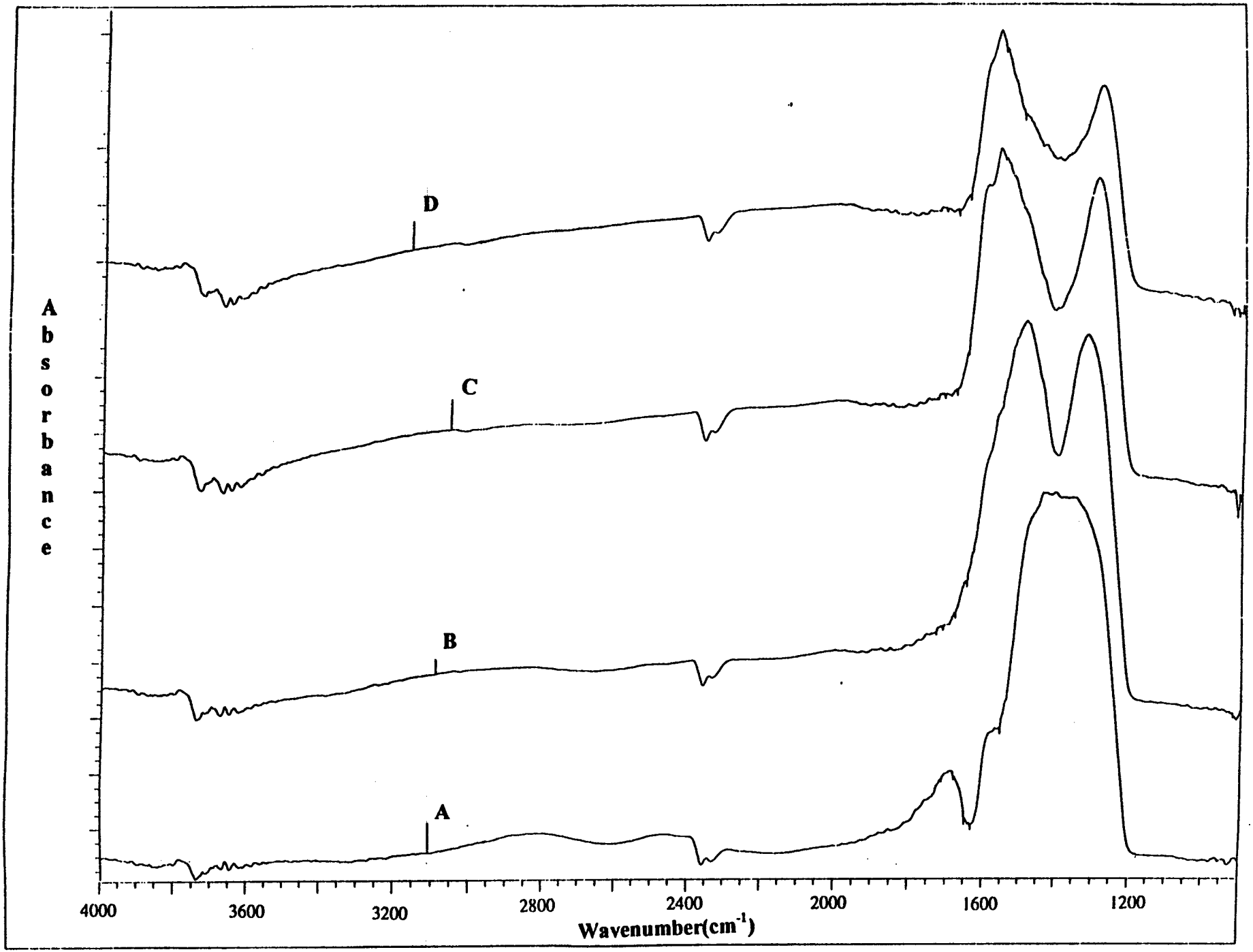
D
C
B
A
Absorbance
4000
3600
3200
2800
2400
2000
1600
1200
Wavenumber(cm-1)

Figure 2

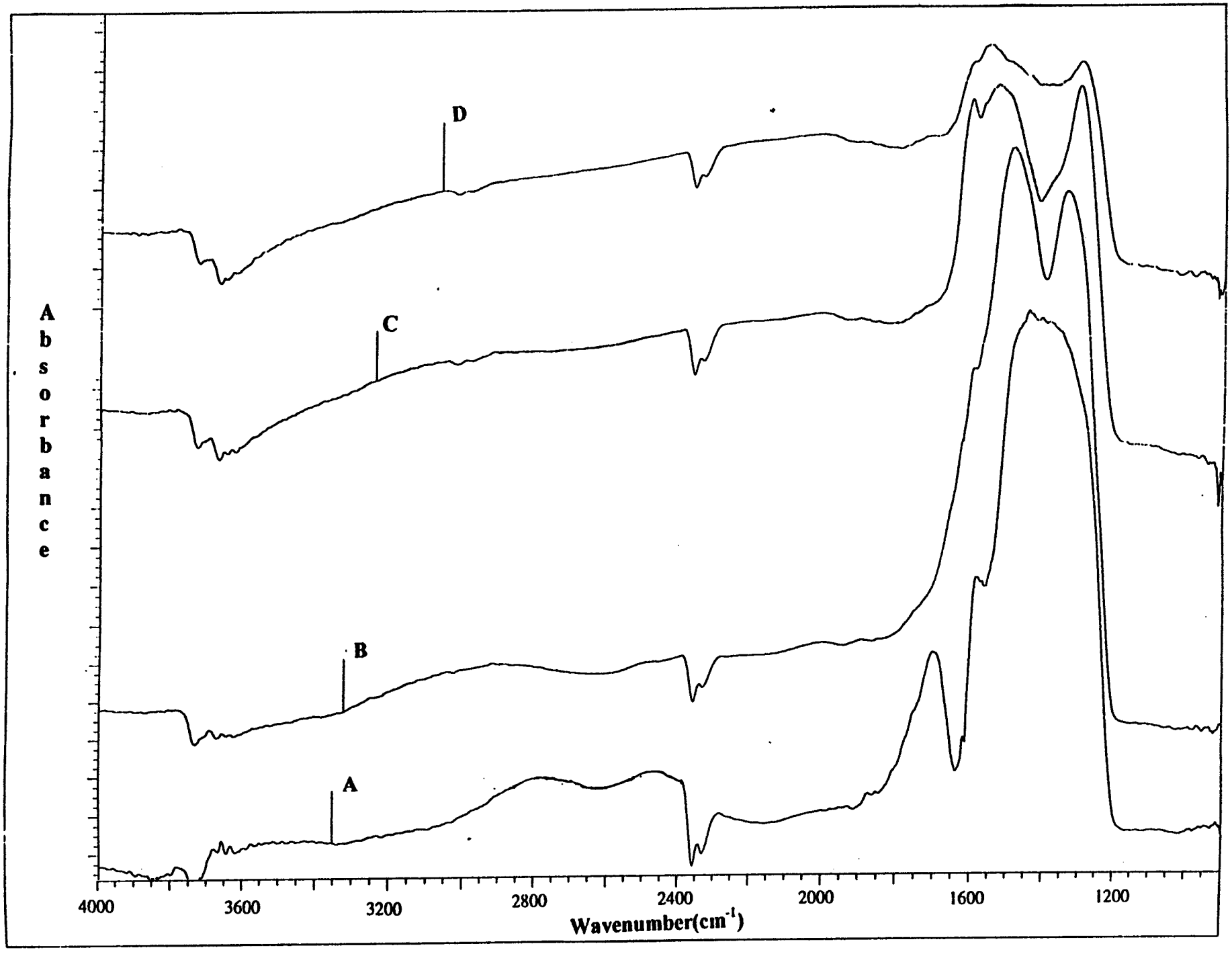
D
C
B
A
Absorbance
4000
3600
3200
2800
2400
2000
1600
1200
Wavenumber(cm-1)

Figure 3

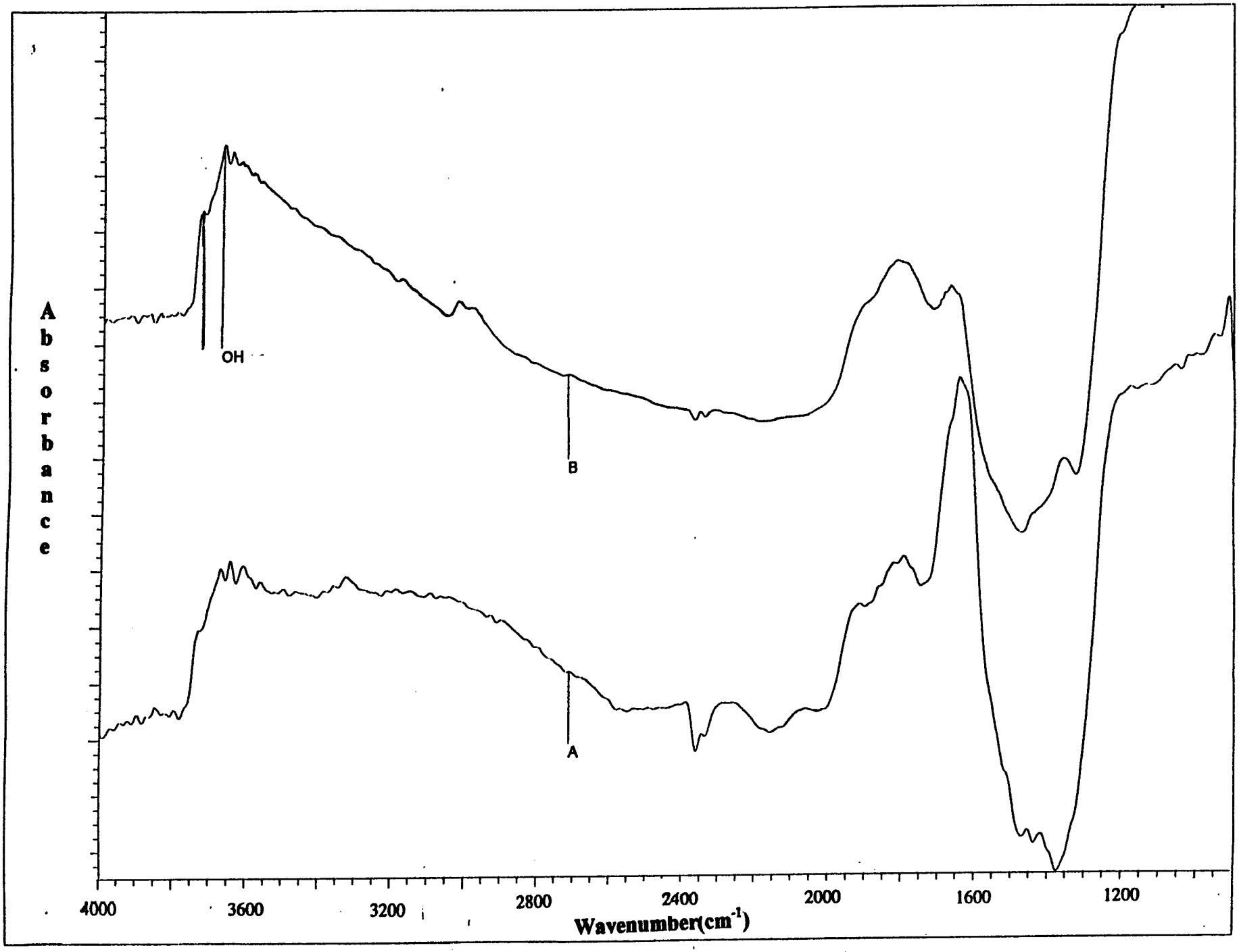
Absorbance
OH
B
A
4000
3600
3200
2800
2400
2000
1600
1200
Wavenumber(cm-1)

Figure 4

Report Number (14) DOE/PC/96206--T1

Publ. Date (11) 199708

Sponsor Code (18) DOE/FE, XF

JC Category (19) UC-101, DOE/ER

DOE